

A Model of Theta Rhythm Production in the Septal-Hippocampal System and Its Modulation by Ascending Brain Stem Pathways

Michael J. Denham^{1*} and Roman M. Borisyuk^{1,2}

¹Centre for Neural and Adaptive Systems, School of Computing, University of Plymouth, Plymouth, UK

²Neural Networks Laboratory, Institute of Mathematical Problems in Biology of the Russian Academy of Sciences, Pushchino, Russia

ABSTRACT: Recent experimental observations have disclosed the existence of a septal-hippocampal feedback circuit, composed of medial septum diagonal band of Broca (ms-dbb) GABAergic projections to the inhibitory interneurons of the hippocampus, and hippocampal GABAergic projections to the ms-dbb, the major targets of which are the GABAergic septo-hippocampal projection cells. We propose that this feedback circuit provides the mechanism for the rhythmic suppression of interneuronal activity in the hippocampus, which is observed as low-level GABAergic-mediated theta activity. We also propose that this circuit may be the mechanism by which ascending brain stem pathways to the ms-dbb, in particular from the reticular formation, can influence hippocampal information processing in response to particular behavioral states, by exercising control over the level and frequency of theta activity in the hippocampus. In support of these proposals, we describe a minimal computational model of the feedback circuit which uses a set of four coupled differential equations describing the average dynamic activity of the populations of excitatory and inhibitory cells involved in the circuit. We demonstrate through simulations the inherently robust 4–6-Hz oscillatory dynamics of the circuit, and show that manipulation of internal connection strengths and external modulatory influences on this circuit changes the dynamics in a way which closely mimics corresponding manipulations in recent neurophysiological experiments investigating theta activity. *Hippocampus* 2000;10:698–716. © 2000 Wiley-Liss, Inc.

KEY WORDS: inhibitory feedback circuit, oscillations, computer modelling, simulations

INTRODUCTION

Oscillatory extracellular field activity in the theta frequency range (5–12 Hz in rodents) has been proposed as playing a fundamental role in information processing in the hippocampus, and hippocampal theta rhythm has been recognized for many years (e.g., Green and Arduini, 1954) as being strongly correlated with specific behavioral activities, e.g., arousal, attention, exploration, and vol-

untary movements. The role of theta during these activities may well be one of facilitating the effect of appropriately timed inputs (Buzsaki and Chrobak, 1995). Freund and Gulyas (1997) suggest that oscillatory suppression of inhibitory interneuronal activity allows the precise timing and synchronization of inhibitory postsynaptic potentials arriving at hippocampal pyramidal cells. Csicsvari et al. (1999) also proposed that oscillating inhibitory networks may provide temporal windows for single cells to suppress or facilitate their synaptic inputs in a coordinated manner.

This relates very closely to our current view of a major role and function of the hippocampus as a monitor of the stability/regularity of the animal's environment, as the animal senses the environment during exploration (Denham and McCabe, 1996; Borisyuk et al., 1999), and in particular to the mechanisms of predictive, contextual learning and recall which we proposed in support of this theory (Denham and McCabe, 1996). These mechanisms require the selective and rhythmical removal and application of inhibition in the areas of the apical dendrites of pyramidal cells where perforant path afferents, and specific excitatory inputs from other hippocampal fields, form synapses. This would have the effect of modifying the ability of these inputs both to selectively change the efficacy of these synapses and to initiate action potentials in the postsynaptic pyramidal cell, as also suggested by Freund and Gulyas (1997).

Others have also implicated the septo-hippocampal interaction as an important mechanism in the control of learning and recall processes in the hippocampus. In particular, Hasselmo and Schnell (1994) and Hasselmo et al. (1995) proposed, based on experimental evidence, that laminar-specific cholinergic modulation by medial septal projections to regions CA1 and CA3 can control both heteroassociative and autoassociative learning mechanisms, respectively, in these regions.

A number of proposals have been made in recent years for the mechanism for the production of theta activity

Grant sponsor: Russian Foundation of Basic Research; Grant number: 99-04-49112.

*Correspondence to: Prof. Michael J. Denham, Centre for Neural and Adaptive Systems, School of Computing, University of Plymouth, Drake Circus, Plymouth PL4 8AA, UK. E-mail: mike@soc.plym.ac.uk

Accepted for publication 6 July 2000

(reviewed in Vertes and Kocsis, 1997; Vinogradova, 1995). In particular it has been proposed that the ms-dbb is the sole source of theta, the so-called "septal pacemaker" hypothesis (Vinogradova, 1995). This conclusion is based mainly on the observation that disconnection of hippocampus from the ms-dbb abolishes hippocampal theta activity, and on the identification of some cells in the ms-dbb as putative endogenous bursting pacemaker cells.

In this paper we describe a septal-hippocampal feedback circuit, based primarily on the anatomical findings of Toth et al. (1993), between the nonpyramidal GABAergic calbindin (CB)-containing hippocampo-septal projection cells in CA1, the GABAergic septo-hippocampal projection cells in the medial septum-diagonal band of Broca (ms-dbb), and their nonpyramidal CB-containing target cells in CA1 of the hippocampus. We propose that this feedback circuit provides a mechanism to the septal pacemaker for the rhythmic suppression of interneuronal activity in the hippocampus which is observed as low-level, GABAergic-mediated theta activity (Vertes and Kocsis, 1997), also sometimes referred to as an atropine-resistant theta activity (Stewart and Fox, 1989a,b). We see the septal-hippocampal feedback circuit both as an alternative to the septal pacemaker hypothesis for the production of this form of theta activity, and as complementary to it, in that our proposal does not contradict the pacemaker hypothesis. Indeed it may reinforce it, insofar as the feedback circuit may provide a synchronizing mechanism for the endogenously rhythmic pacemaker cells in ms-dbb.

We also propose that the hippocampal-septal feedback circuit may be the mechanism by which ascending brain stem pathways to the ms-dbb, in particular from the reticular formation, can influence hippocampal information processing in response to particular behavioral states, by exercising control over the level and frequency of theta activity in the hippocampus, and therefore in particular the timing of inhibition of hippocampal pyramidal cells (Vinogradova, 1995; Vertes and Kocsis, 1997; Kirk, 1998).

To support our proposals, we developed a coarse-grained computational model of the feedback circuit, which uses a set of coupled differential equations of the Wilson-Cowan form (Wilson and Cowan, 1972) to describe the average activity of the populations of excitatory and inhibitory cells involved in the circuit. We use the specific electrophysiological characteristics of the hippocampal inhibitory cell populations in the circuit, as distinguished by their staining properties and thus identified as belonging to the class of CB-containing cells, to set the time constants associated with the dynamics of these populations. Similarly, we set the time constant of the septo-hippocampal projection cell population to be consistent with their identification as belonging to the class of parvalbumin (PV)-containing inhibitory cells. We then investigated the dynamic behavior of the circuit, using the mathematical technique of bifurcation analysis, and show that a stable oscillatory regime exists for a wide range of parameters of the system. We also find that the natural frequency of this oscillation is in the theta range (approximately 6 Hz) and that it stays almost constant under variation of the circuit parameters. On this basis we postulate that 1) this robust oscillation represents the theta rhythm, and 2) that the almost constant frequency of the oscillation is consistent with the hypothesis that variations in theta fre-

quency are due primarily to external modulatory influences from brain stem afferents rather than internal septal-hippocampal mechanisms (Kirk, 1998).

We also investigated the effects of internal connection strengths and external modulatory influences on the oscillatory regime displayed by the circuit. We show the similarity of the results of these simulations to corresponding neurophysiological experimental results describing the effects of various lesions on the amplitude and frequency of the theta rhythm.

ANATOMICAL EVIDENCE FOR THE EXISTENCE OF THE FEEDBACK CIRCUIT

It is known that GABAergic afferents from the ms-dbb innervate most of the GABAergic interneurons in the hippocampus. These relatively sparse afferents can therefore have a powerful disinhibitory control over the activity of the pyramidal cells (Freund and Antal, 1988; Freund and Gulyas, 1997). In their anterograde *Phaseolus vulgaris* leucogglutinin (PHAL) labeling studies, Freund and Antal (1988) found that both CB-containing and parvalbumin (PV)-containing hippocampal nonpyramidal cells were innervated by the septo-hippocampal projections, predominantly in strata oriens and radiatum of CA1 and CA3, and in the hilus and granule-cell layer of the dentate gyrus. In some sections of CA3, as many as 84% of such cells were so innervated, whereas contacts with cells in the CA1 region and in the molecular layer of the dentate gyrus were less frequent. Only very few contacts were made in the stratum lacunosum moleculare of CA1 and CA3.

Alonso and Kohler (1982) showed the existence of hippocampal projections to the ms-dbb, and demonstrated that these projections came almost exclusively from cells in the stratum oriens of the CA1–CA3 regions. These cells appeared to be nonpyramidal on the basis of their laminar distribution. More recently, Gaykema et al. (1991) described the topography of this projection, and Toth and Freund (1992) confirmed its GABAergic nature, together with strong immunostaining of the hippocampal cells for CB. The experimental evidence of Toth and Freund (1992) showed that, following HRP injections into the medial septum, the majority of retrogradely labeled cells in the hippocampus were nonpyramidal, located mainly in the stratum oriens/alveus border of the CA1–CA3 regions, and that 80% of these cells were found to be immunoreactive for calbindin D_{28K}. The remaining 20% were found to be neuropeptide Y (NPY)-immunoreactive cells. Only one PV-containing cell was labeled, in the stratum oriens of CA1.

More recently, Toth et al. (1993), by injection of PHAL mainly into the strata pyramidale and oriens of the CA1 region, found PHAL-labeled axons in both the lateral septum and ms-dbb complex. Labeled axons in the lateral septum are known to originate from hippocampal pyramidal cells (Leranth and Frotscher, 1989), whereas most of the labeled hippocampal boutons in the ms-dbb complex were immunoreactive for GABA, indicating that the origin of these hippocampo-septal projections were GABAergic cells. Recently, Blasco-Ibanez and Freund (1995) showed that the vast

majority of presumed excitatory synapses on the hippocampo-septal projection cells originate from local collaterals of CA1 pyramidal cells, while only a negligible number of synapses were thought to originate from CA3 pyramidal cells. It is therefore likely that the cells receive a highly convergent excitatory input from the local collaterals of CA1 pyramidal cells.

To further examine the target cells of the projections, Toth et al. (1993) combined PHAL tracing with immunostaining for PV and choline acetyltransferase (ChAT). Both ChAT-positive cells and PV-containing cells were found in large numbers throughout the medial septum, and both cell types were among the targets of the hippocampo-septal projections in the ms-dBB. However, most of the projections formed multiple contacts with the cell bodies and dendrites of PV-containing cells, and only occasionally with ChAT-positive cells.

It also appears that the CB-containing nonpyramidal hippocampo-septal projection cells in CA1 have completely different electrophysiological characteristics from spontaneously active and fast-firing PV-containing inhibitory interneurons: they are difficult to activate by afferent stimulation, have low or no spontaneous activity, and have broad action potentials (Kawaguchi and Hama, 1988). They are thus likely to show low firing rates during theta activity and to discharge synchronously with pyramidal cells during sharp wave activity, leading to their possible misclassification as pyramidal cells in extracellular recording experiments (Toth et al., 1993).

Finally, the combination of anterograde PHAL labeling of the targets of hippocampo-septal projections with retrograde horseradish peroxidase (HRP) labeling showed that many septo-hippocampal projection cells in the ms-dBB were the direct targets of hippocampo-septal projections. This provides strong evidence for a direct septal-hippocampal feedback pathway between nonpyramidal, CB-containing (Toth and Freund, 1992) GABAergic cells in the hippocampus, and PV-containing GABAergic cells in ms-dBB.

The anatomical evidence described above suggests the septal-hippocampal feedback circuit shown in Figure 1. This circuit is a modified version of that described by Toth et al. (1993). The modification we have introduced is that we show the main septo-hippocampal projections terminating on the population of CB-containing inhibitory interneurons in CA1, which act as feedforward inhibitory interneurons on CA1 pyramidal cells, rather than on the same population of CB-containing inhibitory cells in CA1 which project to the ms-dBB, as shown in Figure 8 of Toth et al. (1993). This is based on the results of Gulyas et al. (1990), Miettinen and Freund (1992), and Freund and Gulyas (1997), which indicate that the CB-containing CA1 GABAergic interneurons are among the major targets of the GABAergic septo-hippocampal projection. These target cells are driven by an excitatory input derived from the Schaffer collaterals, the excitatory projections from CA3 pyramidal cells to CA1 pyramidal cells. This is based on evidence from Halasy et al. (1996) and Buhl et al. (1994, 1996) that the CB-containing bistratified interneurons in CA1 are activated by Schaffer collateral/commissural axons in such a feedforward manner, and synapse primarily on the CA1 pyramidal cells (Sik et al., 1995; Gulyas and Freund, 1996).

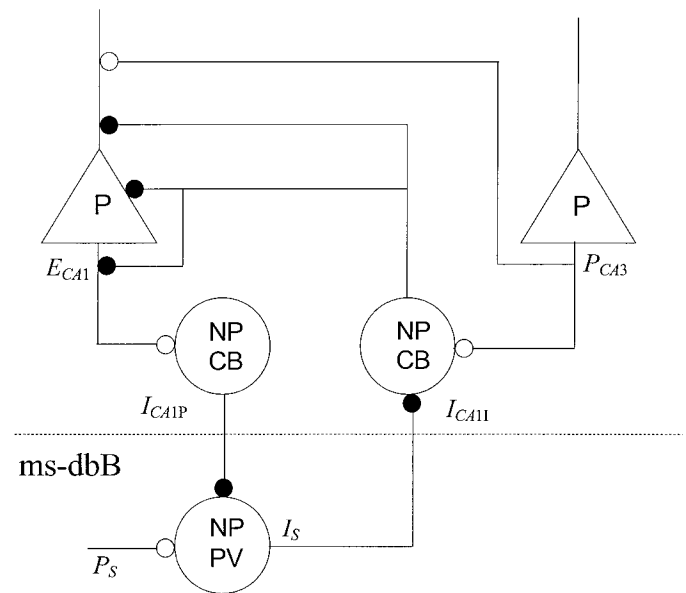


FIGURE 1. Proposed hippocampal-septal inhibitory feedback circuit. P, a pyramidal cell; NP, a nonpyramidal cell; CB, a calbindin-containing cell; PV, a parvalbumin-containing cell; solid circle, an inhibitory connection; open circle, an excitatory connection.

This circuit has two exogenous excitatory inputs: P_{CA3} , the input activity of the CA3 pyramidal cells, via the Schaffer collaterals; and P_s , an external input to the medial septal PV-containing GABAergic cells, which later we identify with the projections from the posterior hypothalamus (PH) and supramammillary nucleus (SUM) to the ms-dBB. The first of these excitatory inputs provides activation of both the excitatory pyramidal-cell population in CA1 and the inhibitory interneuron cell population in CA1. The second excitatory input activates the inhibitory nonpyramidal GABAergic projection cells in ms-dBB.

MATERIALS AND METHODS

The Computer Model

We have modeled the feedback circuit as a set of coupled populations of excitatory and inhibitory cells. The average activity of each population is described by a differential equation of the Wilson-Cowan type (Wilson and Cowan, 1972). The model equations are given by:

$$\tau_{E_{CA1}} \frac{dE_{CA1}}{dt} = -E_{CA1}(t) + (k_e - E_{CA1}(t)) \cdot Z_e(-w_{E_{CA1} \leftarrow I_{CA1P}} I_{CA1P}(t) + P_{CA3}(t)) \quad (1)$$

$$\tau_{I_{CA1P}} \frac{dI_{CA1P}}{dt} = -I_{CA1P}(t) + (k_i - I_{CA1P}(t)) \cdot Z_i(w_{I_{CA1P} \leftarrow E_{CA1}} E_{CA1}(t)) \quad (2)$$

$$\tau_{ICA1I} \frac{dI_{CA1I}}{dt} = -I_{CA1I}(t) + (k_i - I_{CA1I}(t)) \cdot Z_i(-w_{ICA1I \leftarrow I_S} I_S(t) + P_{CA3}(t)) \quad (3)$$

$$\tau_{ISEPT} \frac{dI_S}{dt} = -I_S(t) + (k_i - I_S(t)) \cdot Z_i(-w_{I_S \leftarrow I_{CA1P}} I_{CA1P}(t) + P_S(t)) \quad (4)$$

where $E_{CA1}(t)$ is the average activity of the CA1 pyramidal cell population (i.e., the fraction of cells which are active within a small period of time centred on t), $I_{CA1P}(t)$ is the average activity of the CA1 CB-containing hippocampo-septal projection cell population, $I_{CA1I}(t)$ is the average activity of the CA1 CB-containing interneuron cell population (note the use of P and I respectively in the subscript notation to distinguish between these two inhibitory population variables), and $I_S(t)$ is the average activity of the ms-dBB PV-containing septo-hippocampal projection cell population. The strength of the connection from the population Y to the population X is described by the value of $w_{X \leftarrow Y}$, and is determined by the product of the average number of contacts per cell and the average postsynaptic current induced in the postsynaptic cell from one presynaptic action potential. $P_{CA3}(t)$ is the excitatory activity of the CA3 pyramidal cells, which acts as input to both the CA1 pyramidal cell population and the CA1 CB-containing interneuron cell population. $P_S(t)$ is the excitatory input to the ms-dBB nonpyramidal GABAergic cell population from the PH and SUM.

The $Z_p(x)$ functions, called the response functions, are the proportions of cells firing in a given excitatory ($p = e$) or inhibitory ($p = i$) population for a given level of input activity x . They are represented by monotonically increasing sigmoid type functions, defined by

$$Z_p(x) = 1/(1 + \exp(-b_p(x - \theta_p))) - 1/(1 + \exp(b_p \theta_p)), \quad p \in \{e, i\},$$

where b_p and θ_p are constants. The derivation of this function, with regard to the distribution of firing thresholds in the cell population, or alternatively the distribution the number of afferent synapses per cell, is described in (Wilson and Cowan, 1972). Finally, $k_p = 1/Z_p(\infty)$.

Choice of the Time-Related Parameters in the Model

Each τ parameter in Equations (1)–(4) represents the time constant of the change per unit of time in the proportion of nonrefractory cells in a population which are firing subsequent to receiving subthreshold excitation, in the case of excitatory inputs. In the case of inhibitory inputs, it represents the time constant of the change per unit of time in the proportion of active cells in a population which stop firing in response to receiving subthreshold inhibition. The value of τ in the Wilson-Cowan population model is usually assumed to be comparable with the membrane time constants of the cells in the population (e.g., Tsodyks et al., 1997). The range chosen is normally 10–20 ms. However, both the CB-containing hippocampo-septal projections cells in CA1 and the

CB-containing interneuron target cells of the septo-hippocampal projections in CA1 fall into the general class of bistratified hippocampal GABAergic cells, and Buhl et al. (1996) reported that the membrane time constant for this class of cells in CA1 is in the range 18.6 ± 8.1 ms, approximately twice as long as the PV-containing basket-cell class of inhibitory hippocampal interneurons. We have therefore set the values of τ_{ICA1P} and τ_{ICA1I} , i.e., the time constants for the two CB-containing inhibitory populations in CA1, somewhat higher than usual, to 30 ms.

This choice of 30 ms for τ_{ICA1I} in particular, i.e., for the time constant of the CB-containing inhibitory interneuron population in CA1, is further supported by the experiments of Toth et al. (1997) on the disinhibition of hippocampal pyramidal cells by GABAergic afferents from the septum. They found that CA3 pyramidal cells discharged in response to stimulation of the septo-hippocampal fibres (via the septal disinhibition process) with latencies between 20–80 ms. Here we assume that similar results would be obtained for disinhibition of CA1 cells by septal stimulation. Thus it seems reasonable to assume a latency of 30 ms for the first stage of this process, i.e., septal inhibition of the inhibitory interneuron population in CA1, and thus for the time constant τ_{ICA1P} , and a latency of 30 ms, as discussed below, for the second stage, i.e., inhibition or disinhibition of the CA1 pyramidal cells. This gives a total latency of 60 ms, well within the range observed by Toth et al. (1997). The use of a latency measurement to provide the time constant in the Wilson-Cowan population model is appropriate, since the time constant τ in this model is derived in fact from a first-order approximation to a time delay. That is, if $E(t + \tau)$ is the proportion of cells in the population which are not refractory and which receive at least threshold excitation at time t , the approximation used in the coarse-grained simulation of the model equations is given by

$$E(t + \tau) \approx E + \tau dE/dt$$

i.e., the first-order Taylor series approximation, which yields a first-order differential equation (Wilson and Cowan, 1972).

In the case of the inhibition of the CA1 excitatory population by the CB-containing bistratified interneurons in CA1, the fact that these cells innervate the dendrites of CA1 pyramidal cells, with only a very small number of synapses, if any, on the soma (Halasy et al., 1996), would suggest a slow inhibitory effect of these interneurons on pyramidal cell firing, due to the relatively slow GABA-A receptor decay kinetics (Banks and Pearce, 2000; Banks et al., 1998) observed for such dendritic synapses (decay time constant of 40–50 ms). Alternatively, if we interpret τ_{ECA1} as related to the average time delay before the pyramidal cells start firing again subsequent to the termination of a period of inhibition, then there is evidence that this time delay can be 20–30 ms if the inhibition is elicited by short duration IPSPs, or 50–100 ms for inhibition elicited by the longest duration IPSPs (Thomson et al., 1996). A value of 30 ms for τ_{ECA1} would not therefore seem unreasonable, and perhaps even slightly low. We recognize, however, that this time constant also reflects the rate of activation of the CA1 pyramidal cell population by the excitatory input from CA3 (P_{CA3}) in Equation (1), and it is impossible to separate this from the time constant of inhibition, or inactivation, as discussed above, within

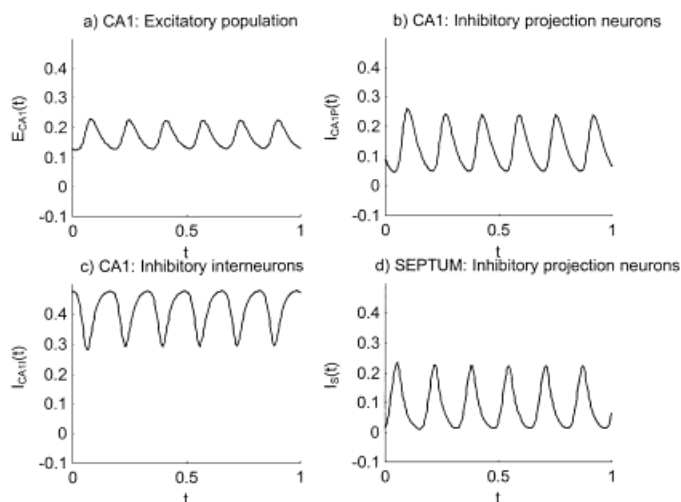


FIGURE 2. Simulation of the model Equations (1)–(4) for the following values of the τ parameters: $\tau_{ECA1} = \tau_{ICA1P} = \tau_{ICA1I} = \tau_{ISEPT} = 30$ ms and $P_S = 5$. Other parameter values as in Table 1.

the Wilson-Cowan form of population activity equation. Thus a compromise value for τ_{ECA1} must be selected for the population activity equation, which also takes this faster time constant into account.

Finally, in the absence of any specific knowledge about the timing characteristics of the inhibition of the ms-dBB PV-containing inhibitory population by the CA1 projection cell population, we have set the value of τ_{ISEPT} also to 30 ms. We have also selected a uniform set of 30-ms values for all time constants in Equations (1)–(4) in order to simplify the model and aid in the understanding of the bifurcation analysis and simulations which we carried out. Using these values, simulations of the circuit model demonstrate a robust oscillation at about 6 Hz (Fig. 2).

However, an alternative, substantially different, setting for the value of the τ_{ICA1P} parameter is suggested by the recent experimen-

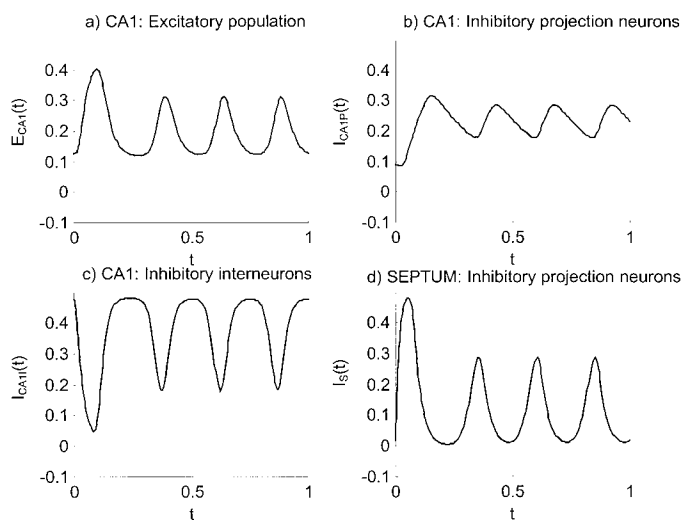


FIGURE 3. Simulation of the model Equations (1)–(4) for the following values of the τ parameters: $\tau_{ECA1} = \tau_{ICA1I} = \tau_{ISEPT} = 30$ ms, $\tau_{ICA1P} = 250$ ms. Other parameter values as in Table 1.

TABLE 1. Parameter Values Used in the Bifurcation Analysis of the Model Equations (1)–(4)

Parameter	$w_{ECA1 \leftarrow ICA1I}$	$w_{ICAP \leftarrow ECA1}$	$w_{ICR1 \leftarrow I_S}$	$w_{I_S \leftarrow ICA1P}$	P_{CA3}	P_S
Value	5	16	8	30	5	4

tal observations of Ali et al. (1998). Using dual intracellular recordings in hippocampal slices, they studied the excitatory postsynaptic potentials (EPSPs) elicited in basket and bistratified interneurons in CA1 by action potentials activated in simultaneously recorded CA1 pyramidal cells. In particular they observed a class of so-called regular spiking (RS) cells, including bistratified cells, which were difficult to distinguish, on the basis of their firing properties, from pyramidal cells. Toth et al. (1993) also noted that the CB-containing hippocampo-septal projection cells in CA1 were, in extracellular recordings, capable of misclassification as pyramidal cells. Ali et al. (1998) found that the RS class included cells which displayed a significant late-firing behavior, in that the firing of the action potential occurred around 260 ms after the onset of the presynaptic excitation. If we were to hypothesize that the CB-containing hippocampo-septal projection neurons in CA1, which are activated by CA1 pyramidal cells, were of this late-firing variety, this would imply a value for τ_{ICA1I} for this population (in Equation (2)) of around 250 ms, again, as above, using the fact that the time constant in the Wilson-Cowan model is actually a first-order approximation to a time delay.

Using this value of τ_{ICA1I} , together with values of 30 ms for the other time constants in Equations (1)–(4), and a higher level of external excitation of the ms-dBB population, simulations of the model show a robust oscillation of about 4 Hz (Fig. 3).

Thus for two quite different, but physiologically reasonable, values of the time constant of the CA1 projection cell population, τ_{ICA1P} , and physiologically justifiable values for the other population time constants in the model Equations (1)–(4), we obtain a robust frequency of oscillation of the model which is representative of the lower range of theta. The other parameter values used in the simulation experiments with the model, which were chosen to be within the oscillatory regime of the model, as determined by a bifurcation analysis (see Results) are listed in Table 1, although, as the latter analysis reveals, the range of parameters for oscillatory operation of the circuit is very large, and the frequency of oscillation remains almost constant over the entire range.

RESULTS

Analysis of the model by simulation experiments shows that there exists a wide range of parameters values for the interconnection strengths $w_{X \leftarrow Y}$ between the populations, for which the circuit displays oscillatory behavior with a natural frequency in the lower end of the theta range (either 4 or 6 Hz). In particular, from

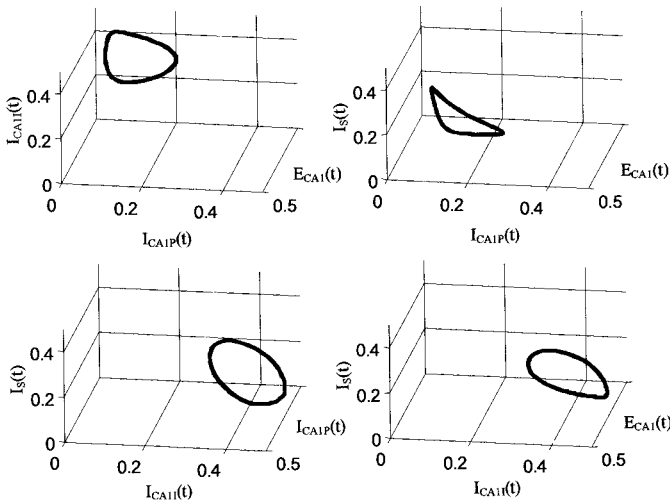


FIGURE 4. Phase space diagrams showing the limit cycle behavior of the septal-hippocampal feedback circuit model (Equations (1)–(4)), for the following values of the τ parameters: $\tau_{E_{CAI}} = \tau_{I_{CAIP}} = \tau_{I_{CAII}} = \tau_{I_{SEPT}} = 30$ ms and $P_S = 5$. Other parameter values as in Table 1.

a bifurcation analysis of the nonlinear dynamic system described by Equations (1)–(4), we found that nonlinear oscillations (limit cycle) can arise only through an Andronov-Hopf bifurcation, when the stable equilibrium point loses stability and a small limit cycle appears near this point, representing the oscillatory behavior of the variables of Equations (1)–(4). This limit cycle behavior is illustrated in the simulation of the model equations shown in phase space diagram from in Figure 4.

The bifurcation analysis was carried out using two active parameters (keeping all other parameters fixed at the “baseline” values in Table 1); the results of this analysis, for the two alternative settings of the τ parameters of the model, as described above, are illustrated in Figures 5 and 6. Figure 5a,b shows the bifurcation curves for pairings of the values of each connection strength parameter $w_{Y \leftarrow X}$ with the value of the external input P_S to the ms-dBB inhibitory population, for the two choices of the τ parameters in the equations, as described above. Figure 6a,b shows the bifurcation curves for pairings of the values of each connection strength parameter $w_{Y \leftarrow X}$ with all other connection strength parameters, for the two choices of the τ parameters. The external input P_S parameter was selected in particular for analysis, with regard to the neurophysiological experimental results which we describe in the Discussion.

In each case the curve shown corresponds to a supercritical Andronov-Hopf bifurcation. This curve separates the regions of stable equilibrium and unstable equilibrium. In the latter region, a stable limit cycle exists for each pair of parameter values. We have also shown through extensive simulation experiments that within this region there exist no further bifurcations of the limit cycle. Thus the limit cycle which appears on entry to this region remains stable and only disappears on exit from the region through the bifurcation curve. An important feature of the Andronov-Hopf bifurcation is that near the bifurcation point, the amplitude of the oscillation, i.e., the size of the limit cycle, is small and grows

quickly from zero as the square root of the distance in parameter space from the bifurcation point. Figures 5 and 6 also demonstrate that the limit cycle behavior of the circuit exists for a very wide range of the parameters of the model.

In the region of stable equilibrium, i.e., at all points outside of the region in which the stable limit cycle exists, the system remains constant at a steady background, or baseline, level of activity. In

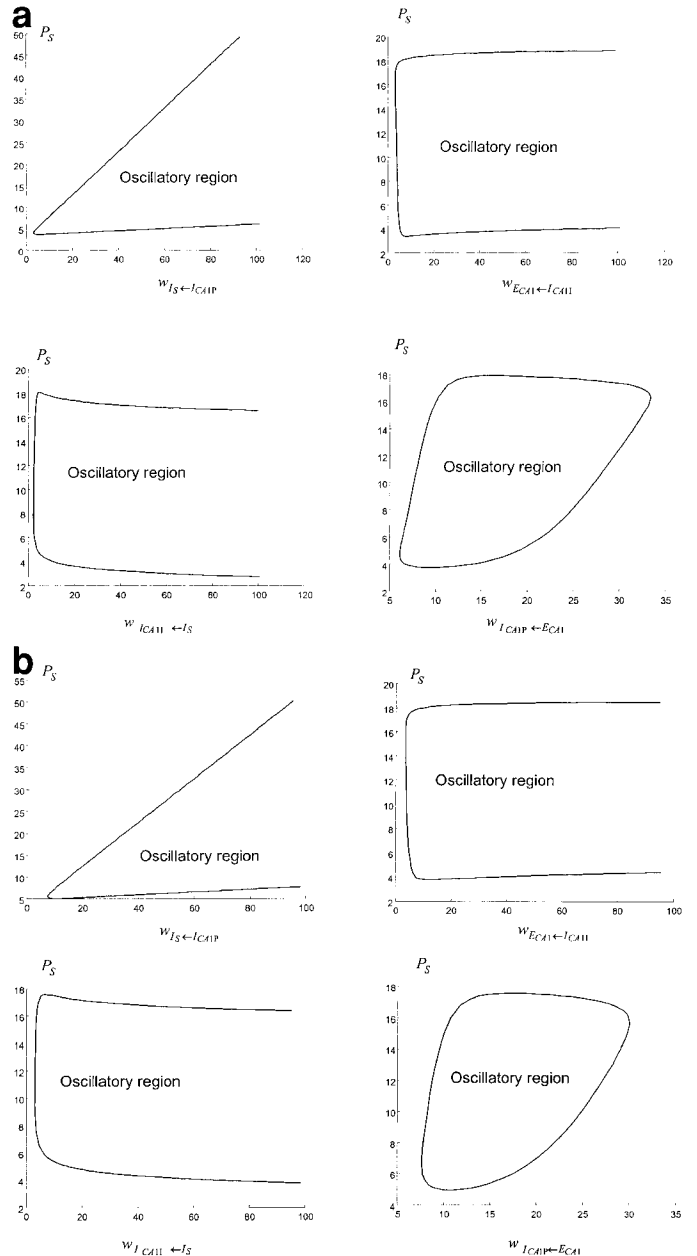


FIGURE 5. a: Bifurcation diagrams with respect to the value of the external excitatory input P_S to the ms-dBB, in the model Equations (1)–(4), for the following values of the τ parameters: $\tau_{E_{CAI}} = \tau_{I_{CAIP}} = \tau_{I_{CAII}} = \tau_{I_{SEPT}} = 30$ ms. Other parameter values as in Table 1. b: Bifurcation diagrams with respect to the value of the external excitatory input P_S to the ms-dBB, in the model Equations (1)–(4), for the following values of the τ parameters: $\tau_{E_{CAI}} = \tau_{I_{CAII}} = \tau_{I_{SEPT}} = 250$ ms. Other parameter values as in Table 1.

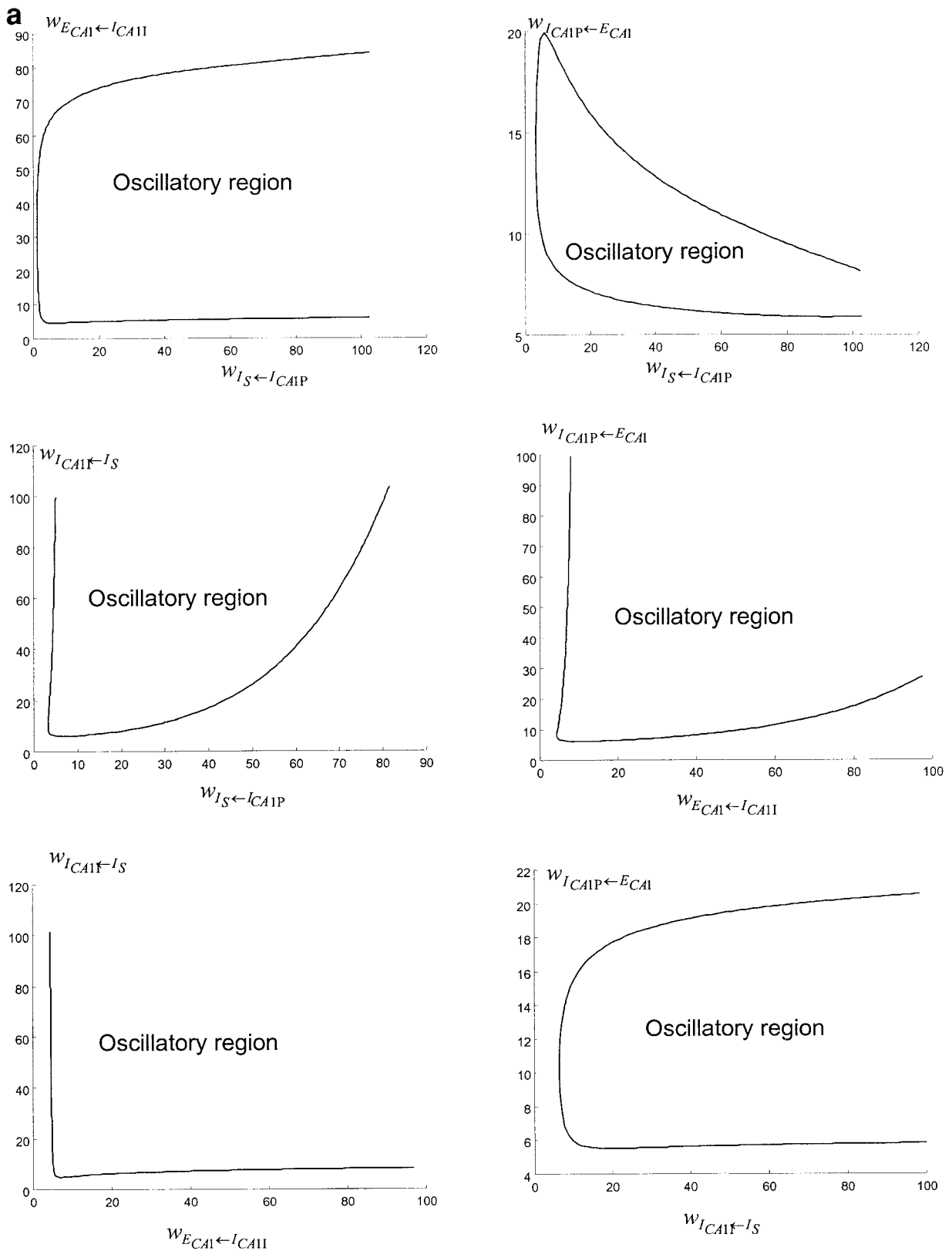


FIGURE 6. a: Bifurcation diagrams for connection parameters in the model Equations (1)–(4), for the following values of the τ parameters: $\tau_{ECA1} = \tau_{ICA11} = \tau_{ISEPT} = 30$ ms. Other parameter values as in Table 1. **b:** Bifurcation diagrams for connection parameters

in the model Equations (1)–(4), for the following values of the τ parameters: $\tau_{ECA1} = \tau_{ICA11} = \tau_{ISEPT} = 30$ ms; $\tau_{ICA1P} = 250$ ms. Other parameter values as in Table 1.

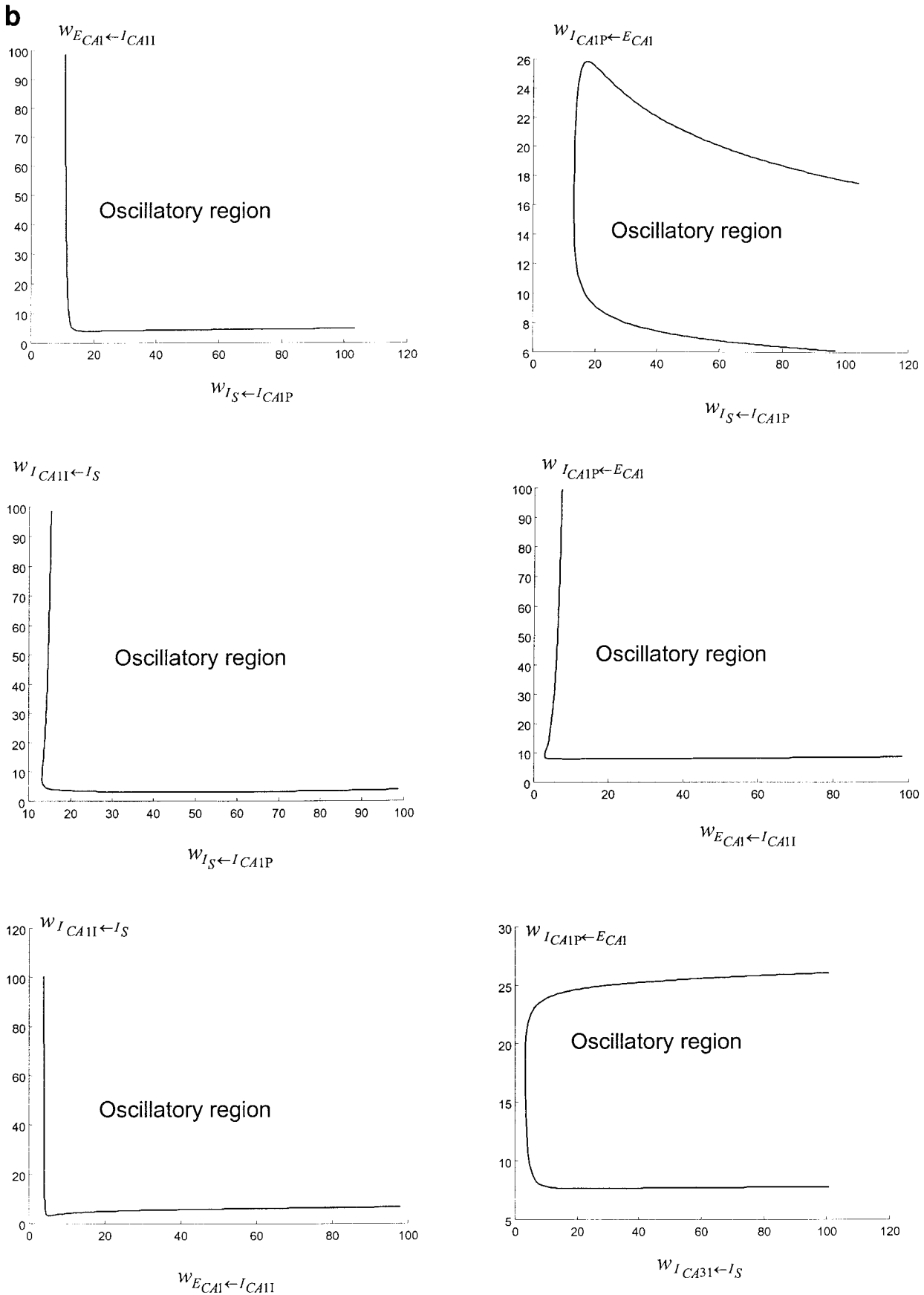


FIGURE 6. (Continued)

general this activity will be nonzero, except in the case where one or more of the parameters of the model are set to zero. Even where the bifurcation curves show an upper limit to the region of stable limit cycle behavior for a given parameter, the stable equilibrium condition still holds in the region where the parameter value exceeds this, e.g., in Figure 6a, at the point (90, 80) on the graph of the bifurcation curve for the parameter pair $w_{I_S \leftarrow I_{CAIP}}$ vs. $w_{I_{CAIP} \leftarrow I_S}$.

It is interesting to note that the imaginary part of the complex eigenvalues of the model equations along the Andronov-Hopf bifurcation curve is almost constant. This means that the frequency of the limit cycle which arises from the Andronov-Hopf bifurcation does not change significantly, having an almost constant value of approximately 4 or 6 Hz, depending on the choice of τ parameters. Also, we calculated the frequency for several parameter values inside the region where the limit cycle exists, and have found that the frequency in this region, and thus over a remarkably and unusually wide range of model parameters, is also almost constant at about 4 or 6 Hz.

In summary, using the methods described in Borisyuk and Kirillov (1992), and briefly in the Appendix to this paper, bifurcation analysis of the model described by Equations (1)–(4) shows that the inhibitory feedback circuit can reliably display an almost constant frequency limit cycle oscillation, at the lower end of the theta range, for a wide range of parameter values. For all parameters outside of this range, the circuit displays a steady background level of activity.

Ability of the Model to Replicate the Effects of Physiological Experiments

In further support of the proposal that the oscillatory behavior of the model is the analogue of the hippocampal theta rhythm, and thus the hypothesis that the septal-hippocampal feedback circuit is a mechanism for the production of GABA-mediated theta activity, we now describe a number of experimental results which have been obtained in recent years, involving various manipulations of the septal-hippocampal system and its ascending pathways from brain-stem regions, in particular the reticular formation. We show that functionally equivalent manipulations of the model (Equations (1)–(4)) of the septal-hippocampal feedback circuit result in changes in oscillatory behavior of the model which closely mimic those changes, in particular in the amplitude and frequency of hippocampal theta, which have been experimentally observed.

Intraseptal Infusion of Muscimol

Bland et al. (1996) showed that microinfusion of the GABA-A agonist muscimol into the medial septum/vertical limb of the diagonal band of Broca of urethane-anesthetized rats resulted in a progressive reduction in the amplitude of theta field activity, and finally its total loss. However, importantly, the frequency of theta field activity remained unaffected throughout the period up to disappearance of theta. Bland et al. (1996) suggested that the decrease in theta field activity and cell discharge rates which they observed could be mediated by the GABAergic septo-hippocampal projection.

The principal GABA receptors in the ms-dBB are GABA-A/BDZ receptors. Agonist-induced activation of this receptor, e.g., through injection of muscimol, either hyperpolarizes the postsynaptic membrane or reduces the level of an existing depolarisation (Walsh et al., 1993). In our model, we propose that the functional equivalent of this experiment is to reduce the magnitude of the external excitatory input P_S from the ascending brain-stem pathways to the nonpyramidal PV-containing GABAergic cell population in the ms-dBB. The effects of this, as predicted by the bifurcation analysis (Figs. 5, 6), are: 1) while the value of P_S remains in the region of oscillatory behavior, a reduction in the amplitude of the oscillations of the circuit as this value approaches the bifurcation curve, but with no change in frequency; and 2) an eventual disappearance of the oscillations as the value of P_S reaches and passes through the bifurcation curve. This effect is confirmed by the simulations shown in Figure 7, which show a reduction in amplitude, but no change in frequency, of the oscillations observed as a result of reducing the value of P_S by about 10%.

Modulation of Theta by Brain Stem Inputs to ms-dBB

It is well-known that afferents to the ms-dBB from the brain stem are of critical importance in determining the frequency of theta (Vinogradova, 1995; Vertes and Kocsis, 1997; Kirk, 1998), in particular the brain-stem-synchronizing pathway originating in the pons region and ascending to the medial septum via the midline posterior hypothalamic region (Bland et al., 1994). Theta activity has been shown to be evoked by stimulation of the reticular formation (RF) and its ascending pathways in the hypothalamus, which reproduces the normal physiologically observed increase in activity of RF neurons during hippocampal theta states, i.e., arousal by sensory stimuli, exploratory activity, and REM sleep. A gradual increase in the intensity of stimulation causes a corresponding linear increase in the frequency of theta (up to 9–10 Hz) and increases the synchrony of theta bursts (Vinogradova, 1995).

During theta, tonically firing cells of the nucleus reticularis pontis oralis (RPO) of RF activate cells of the SUM, which converts this steady barrage into a rhythmical pattern of discharge which is then relayed to the GABAergic and cholinergic cells of the ms-dBB (Vertes and Kocsis, 1997). These SUM afferents to ms-dBB form synapses which are most likely to be excitatory, with both the PV-containing GABAergic cells and the cholinergic cells (Borhegyi et al., 1998). SUM cells fire rhythmically phase-locked to the concurrent hippocampal theta, and it has been suggested that they may participate in its modulation by mediating the frequency component of reticularly elicited theta activity (Borhegyi et al., 1998). It is also the case that this rhythmic response of the SUM to RPO stimulation was not abolished when theta activity in the hippocampus was eliminated by procaine injection into the septum (Kirk et al., 1996), thus indicating that the rhythmic discharge of SUM cells during hippocampal theta is independent of theta activity in the septal-hippocampal system.

It has also been observed that transection of the brainstem afferent connections have different effects at different levels of the transection. At rostromedial, midcollicular, and precollicular levels,

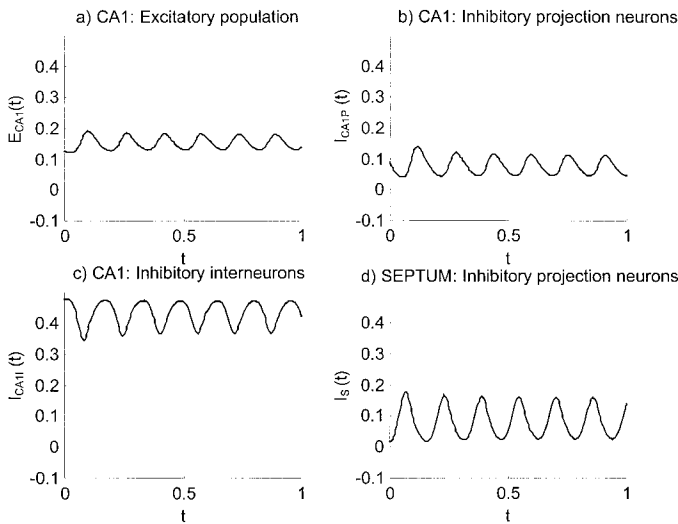


FIGURE 7. Simulation of the model of the septal-hippocampal feedback circuit (Equations (1)–(4)), in which the value of the constant external excitatory input P_S to the ms-dBB nonpyramidal cell population has been reduced to 4.5, compared to a value of 5 for the simulation shown in Figure 2. Other parameter values are as for Figure 2.

disconnection of the septum from brain-stem structures caudal to the SUM results in a low-frequency (3.5–4.0 Hz), nearly continuous theta. Only transection at the level of the posterior hypothalamus results in the total elimination of hippocampal theta (reviewed by Vinogradova, 1995; Vertes and Kocsis, 1997).

The suggestion has therefore been made that the frequency of theta rhythm is encoded and primarily determined in the SUM, and not in the septum, as part of an ascending system for modulating theta, with the posterior hypothalamic nucleus (PH) acting in synergy with the SUM as two relays in an ascending “theta-synchronizing” system from the RPO to the ms-dBB (Kirk et al., 1996). The PH, however, is more involved in the release and amplitude modulation of theta than in determining the frequency of theta (Kirk and McNaughton, 1993; Kirk, 1998). It appears that theta-related PH cells discharge tonically during hippocampal theta, whereas theta-related SUM cells discharge rhythmically and phase-locked to concurrent hippocampal theta activity (Kirk et al., 1996). Lesions of, or procaine injected into, the PH, abolish hippocampal or septal theta activity (Bland et al., 1995), whereas procaine infused into the SUM attenuates the amplitude (by about 60%) and frequency (from 6.5 Hz to 4 Hz) of reticularly elicited hippocampal theta in urethane-anaesthetized (Kirk and McNaughton, 1993; Thinschmidt et al., 1995) and unanaesthetized (McNaughton et al., 1995) rats. Lesions of the SUM do not appear to have any affect on spontaneous or movement-related theta, as opposed to reticularly elicited theta, in the unanaesthetized rat (Thinschmidt et al., 1995).

We simulated the experimental observations described above by introducing a sinusoidal component to the external input P_S to the ms-dBB population of cells in our model, i.e., $P_S(t) = A + B \sin(\omega t)$, $A = 15$; $B = 5$. This emulates the combination of a tonic PH input and a phasic SUM input. Selecting ω to be at a

higher frequency than the natural frequency of the feedback circuit entrains the period of the circuit oscillations to that of the input signal. This is shown in Figure 8, where the sinusoidal component of the input P_S is at a frequency of 10 Hz.

Our experience with the model is that, for a constant value, e.g., of 15, for A and B (mean level and amplitude) of the sinusoidal input to the medial septum cell population, the amplitude of the oscillatory response of the CA1 pyramidal cell population decreases rapidly with increasing frequency of this input signal. The amplitude is about 70% at 12 Hz and 20% at 20 Hz, of that at 10 Hz (the frequency shown in Fig. 8). Increasing the amplitude and mean level of the sinusoidal input from 15 to 30 makes this falloff in CA1 pyramidal-cell oscillation amplitude even greater, the amplitude at 20 Hz in this case being only 5% of that at 10 Hz. Values of A and B below ~ 8 fail to entrain high-frequency oscillations.

In summary, there is a narrow range of amplitudes of the sinusoidal input to the medial septal population in the model for which entrainment of the oscillations of the CA1 pyramidal population to higher frequencies is possible (~ 8 –30 Hz) for the set of model parameters given in Table 1, and all the time constants set at 30 ms. The amplitude of the entrained CA1 oscillations falls off rapidly with increasing frequency of stimulation, and this effect is increased for higher-amplitude input signals.

From the model Equations (1)–(4), and from the bifurcation curves in Figures 5 and 6, it follows that elimination of the entire external excitatory input P_S to the ms-dBB nonpyramidal population (i.e., setting $P_S = 0$) will result in a total loss of the oscillatory activity in the model, since without any form of excitatory input, the activity I_S of the ms-dBB nonpyramidal cell population, as described by Equation (4), will decay to, and remain at, zero. This corresponds to the experimental manipulation described above in which the ascending pathway to the ms-dBB is transected at the level of the SUM or PH (Vinogradova, 1995).

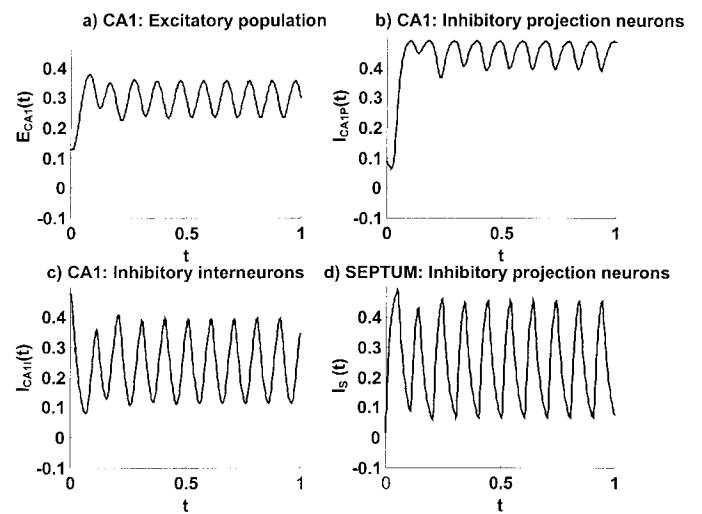


FIGURE 8. Entrainment of the oscillations of the model Equations (1)–(4) by an external oscillatory input P_S to the ms-dBB septo-hippocampal projection population, at a frequency f of 10 Hz. Parameter values as in Table 1, except $P_S(t) = 15(1 + \sin 2\pi ft)$, with all time constants equal to 30 ms.

If only the periodic component of the input P_S to the ms-dBB is eliminated, with a constant excitatory input maintained, then any externally elicited, higher-frequency, entrained oscillatory activity of the model obviously will be eliminated, and the oscillatory activity will revert to the lower, natural frequency of the feedback circuit (as in Figs. 2, 3), which, with our two selections of the τ parameters in the model Equations (1)–(4), corresponds to a frequency of about 4 or 6 Hz, respectively. This, we suggest, corresponds to the experimental cases of procaine injections into SUM (Kirk and McNaughton, 1993; Thinschmidt et al., 1995; McNaughton et al., 1995), the effect of which, we assume, is to selectively eliminate the rhythmic, phasic activity of SUM cells, leaving the tonic input from PH intact.

DISCUSSION

In this paper we have 1) proposed that the septal-hippocampal feedback circuit we describe is a mechanism for the production of low-level GABAergic, interneuron-mediated hippocampal theta activity; 2) described a coarse-grained population activity-based computational model of this circuit and demonstrated its dynamic properties through bifurcation analysis via simulation of the model; 3) shown that these dynamic properties are highly consistent with the proposal that the circuit is a mechanism for the production of theta activity; and 4) shown that various manipulations of the model, which mimic experimental manipulations of the biological circuit, influence the oscillatory dynamics of the circuit in a manner consistent with the effect that these experiments have on hippocampal theta activity. These manipulations include intraseptal infusion of the GABA agonist muscimol, and procaine injections and lesions of the ascending brain-stem nuclei, the posterior hypothalamus (PH), and the supramammillary nucleus (SUM), which send afferents to the ms-dBB and have been postulated as the main components of a theta-controlling system from the RPO to the ms-dBB.

In particular, we investigated the dynamic behavior of the hippocampal-septal feedback circuit, using bifurcation analysis, and we showed that a stable oscillatory regime exists for a wide range of parameters of the circuit. We also found that the frequency of this oscillation stays almost constant under variation of the parameters, and, for a physiologically reasonable choice of time parameters in the model, the frequency is about 6 Hz. On this basis we postulate that 1) this robust oscillation represents the low level “residual” theta rhythm maintained by the GABAergic septo-hippocampal projections which remains after the selective and total elimination of cholinergic ms-dBB projections to the hippocampus (Stewart and Fox, 1989a,b; Lee et al., 1994; Vertes and Kocsis, 1997), and 2) that the almost constant frequency of the oscillation is consistent with the hypothesis that variations in theta frequency are due primarily to external modulatory influences from brain stem afferents (Kirk, 1998).

Further support for our proposal is based on the phase relationships between the oscillatory activity in each of the populations in

the septal-hippocampal feedback circuit. In particular, the simulations of the model shown in Figures 2 and 3 show that the ms-dBB PV-containing nonpyramidal cell population oscillates with a phase advance of approximately 62° relative to the CA1 pyramidal-cell population. This appears to be consistent with the experimental results of Bland et al. (1999). In simultaneous recording of septo-hippocampal cell pairs which showed rhythmic activity during hippocampal theta, the rhythmic bursts of the so-called medial septum theta-ON cells, phase-locked to theta, precede those of the CA1 hippocampal theta-ON cells by about $90\text{--}100^\circ$ (Fig. 2 of Bland et al., 1999) of the theta period. They also showed, from a correlation between the septal-cell activity and the hippocampal theta field activity, the former lagging behind the latter by about 70° . Since hippocampal field activity was recorded from the molecular layer of the dentate gyrus, the CA1 hippocampal activity would be expected to be in 180° phase shift with this, resulting in a phase lead of the septal activity over the CA1 hippocampal activity of about 110° , consistent with the above result. In our model, we demonstrate (Fig. 2) a phase lead of approximately 65° , which is within a reasonable range of the experimental result given the coarse-grained nature of the model.

Relationship to Existing Theories of Hippocampal Theta Production

Previous work related to our proposals starts with that of McLennan and Miller (1974), who proposed a mechanism for theta production which also involved a feedback system between septum and hippocampus. However, their circuit differed considerably from that which we propose. In their circuit, McLennan and Miller (1974) suggested the existence of a recurrent collateral inhibitory circuit located in the lateral septum region, under excitation from the hippocampus via the fimbria. They proposed that neural activity in the hippocampus is responsible, through projections to the lateral septum, for the generation of phasic activity in the lateral septum, mediated by this recurrent circuit. Projections from the lateral septum to the medial septum are then responsible for the rhythmic discharge exhibited by medial septum neurons, which is then projected back to the hippocampus. They also proposed that a direct inhibitory input to the medial septum from the hippocampus, via the fimbria, serves to synchronize the rhythmic discharge of the medial septum neurons, by a “reset” mechanism which originates in the hippocampus. This form of feedback circuit, from the hippocampus via the lateral septum, medial septal, and back to the hippocampus, which generates the rhythmic activity in the lateral septum, and transmits it to the medial septum and thence back to the hippocampus, with an additional synchronizing input from hippocampus direct to the medial septum, must now be viewed as less likely to be a source of theta, since the lateral to medial septum projection has been shown to be sparse in the rat (Leranth et al., 1992; Witter et al., 1992), as well as in the guinea pig and monkey. This theory was further promoted in McLennan and Miller (1976), where it was reported that ipsilateral sections of the fimbrial input to the septum from the hippocampus, which include the projections to both the medial and lateral septum described above, almost completely eliminated (in all but 2 out of 11

neurons) the rhythmic bursting discharge pattern normally exhibited by medial septum neurons.

Stewart and Fox (1989a) tested the idea that a hippocampal-septal feedback circuit is responsible for the production of theta. They reported that cooling the fimbria/fornix reversibly eliminated the hippocampal theta rhythm, but had no effect on 21 out of 25 rhythmic ms-dBB cells tested. Out of the 4 cells that lost their rhythmicity during cooling, 2 were tested with atropine and were found to be atropine-resistant, i.e., GABAergic cells. However, atropine-resistant cells were also found among those cells which maintained rhythmic firing during cooling of the fimbria/fornix. This seemed to indicate that these cells and the cholinergic (termed the atropine-sensitive by Stewart and Fox, 1998a) cells in ms-dBB which Stewart and Fox (1998a) were mainly observing do not depend on the periodic output from the hippocampus for their rhythmic firing.

In follow-up work, Stewart and Fox (1989b) showed that injections of large doses of atropine produced an almost complete loss of theta, but that a "residual theta rhythm" (i.e., theta that could not be detected by conventional techniques) was uncovered by triggering the hippocampal EEG on the ms-dBB neurons that continued to fire rhythmically in the absence of theta. Since atropine completely blocked septal cholinergic influences on the hippocampus, it was reasoned that residual theta was mediated by rhythmically firing GABAergic septo-hippocampal neurons. Supporting this conclusion, Lee et al. (1994) demonstrated in behaving rats that the selective and total elimination of cholinergic ms-dBB projections to the hippocampus significantly reduced the amplitude of, but did not eliminate, hippocampal theta, leading to the conclusion that low-amplitude theta was maintained by GABAergic septo-hippocampal projections.

This raises the questions: 1) did the fimbria/fornix cooling in the Stewart and Fox (1989a) experiment completely eliminate theta, or, as in the later Stewart and Fox (1989b) experiments, did a residual GABAergic-mediated theta remain; and 2) if a residual theta was still present, did the GABAergic septo-hippocampal projections remain intact during cooling, as the results of Lee et al. (1994) suggest must be the case? If some of these projections did remain intact, then continuing rhythmic activity of GABAergic cells, produced by the septal-hippocampal feedback circuit, during the cooling experiment, is feasible, although, we admit, unlikely with such weakened connections.

At present, however, the most popular theory for the production of hippocampal theta is the existence of so-called medial septal "pacemaker" neurons (Petsche et al., 1965; Stumpf, 1965; Vinogradova, 1995; Vertes and Kocsis, 1997), i.e., rhythmically discharging neurons, which have been shown by Vinogradova (1995) to retain their rhythmic, pacemaker-like, discharge patterns in the case of partial or complete lesions of the afferent projections to the ms-dBB, strengthening the case that these neurons are the sole source of theta activity. We make the strong point here that while we propose that the septal-hippocampal feedback circuit which we have identified and modeled can in itself produce the rhythmic activity which is observed as theta activity, this does not rule out the possibility that a major function of the circuit may well be to enhance the effect of the septal pacemaker neurons. Indeed,

Petsche et al. (1965) observed that rhythmically discharging medial septum neurons do not fire in perfect synchrony, and a role of the feedback circuit may be to impose synchrony on the endogenous rhythmic activity of these cells.

In this paper, we have proposed the septal-hippocampal feedback circuit principally as the mechanism for the rhythmic suppression of interneuronal activity in the hippocampus which is observed as low-level theta activity (Vertes and Kocsis, 1997). That is, we are concerned with only the component of theta activity mediated by the rhythmically bursting GABAergic ms-dBB neurons, rather than that mediated by the cholinergic, atropine-sensitive cells in ms-dBB. However, since the cholinergic and GABAergic cells are interconnected (Brauer et al., 1998), it is likely that if either class of ms-dBB cells has endogenous rhythmic behavior, then this will also be observable in the other class. Thus we do not rule out the possibility that the GABAergic cells, as well as the cholinergic, atropine-sensitive cells, in ms-dBB will continue some form of rhythmic bursting behavior in the absence of feedback from the hippocampus, as might be the case in cooling of the fimbria/fornix, i.e., our proposal does not directly contradict the hypothesis that there are cells in ms-dBB which are intrinsically rhythmic and do not depend on hippocampal input for their rhythmicity.

Indeed, if we consider the cholinergic cells to constitute the majority of rhythmic bursting cells in the ms-dBB (Apartis et al., 1998) and we regard their projections to the ms-dBB GABAergic cell population in the current model as an excitatory periodic input to this population, the simulated oscillatory behavior of this resulting, very simplified, model of the feedback circuit superimposed on an intrinsic "septal pacemaker" would be identical to that shown in Figure 8, where we postulated rather than the periodic input was from the ascending brain-stem inputs to the medial septum. Thus it is shown that the feedback circuit could indeed serve principally to synchronize the action of intrinsically rhythmic pacemaker cells in the ms-dBB. However, a more detailed model, which incorporates the interaction between two ms-dBB cell populations, in particular the cholinergic activation of the GABAergic cell population and the postulated rhythmic inhibition of the cholinergic ms-dBB cells by the GABAergic ms-dBB cells (Lee et al., 1994; Brazhnik and Fox, 1997), is necessary to fully simulate and demonstrate this behavior.

It is interesting to note that others may well have considered the interaction of excitatory and inhibitory cell populations in the septal-hippocampal system as a mechanism for production of theta-related rhythmic activity, but have discarded the hypothesis as a result of failure to obtain sufficiently low-frequency oscillations in the theta range, using physiologically plausible membrane time constants in the population equations. Our results in this respect may differ from previous attempts in this direction in two respects: 1) the model involves a chain of four cell populations in the feedback circuit, which theoretically and empirically extends the overall period of the circuit oscillations, compared to, say, two reciprocally interconnected populations; and 2) recent physiological experiments have revealed a large variety of nonpyramidal cell types in the hippocampus and a correspondingly wide range of electrophysiological characteristics of these cell types (e.g., Ali et

al., 1998), including membrane time constants and postsynaptic potential decay rates. Such a wide variation in these characteristics, and in the interconnectivity patterns of interneuronal populations, offers the possibility that different cell types can participate in a range of feedback circuits which are capable of generating frequencies of oscillations ranging from theta to the 200-Hz ripples observed in CA1 during slow-wave sleep and quiet wakefulness.

Relationship to Previous Work on Septo-Hippocampal Feedback Inhibition

As originally suggested by Hasselmo and Schnell (1994) and Hasselmo et al. (1995), a septo-hippocampal inhibitory feedback circuit appears to be an essential mechanism for the matching process in CA1 and the learning/recall processes in CA3 which would be necessary to support a familiarity vs. novelty detector role for the hippocampus. In this case, however, inhibition is mediated by cholinergic afferents from medial septum, through the mechanisms of enhancement of currents mediating adaptation, and suppression of intrinsic excitatory synaptic transmission. In the present paper, however, we explore the possibly complementary role of the direct hyperpolarizing effect of the GABAergic projections from ms-dBB on the inhibitory interneurons in the hippocampus as a feedback mechanism for rhythmically controlling the dynamics of learning in CA1 and CA3.

A possible computational role for this theta-frequency rhythmic inhibition of interneurons by septal projections is examined in Hasselmo et al. (1996) and Sohal and Hasselmo (1998a,b). The role proposed by Sohal and Hasselmo (1998a,b) is one of improving disambiguation in the retrieval of sequence memories, where the sequences have the same starting point. The model used to examine this was an analogue network model of region CA3, and the effect of the theta rhythm was to rhythmically change the level of GABA_B suppression of synaptic transmission in recurrent connections in the network. The role proposed in Denham and McCabe (1998) for the rhythmic inhibition of synaptic transmission in the hippocampus was a somewhat simpler one: that of resetting the cycle of predictive learning in CA3 to limit the prediction time to the theta period. This follows from the somewhat different role assigned to CA3 in Denham and McCabe (1998), as a predictive learning network underlying familiarity/novelty detection, rather than as a sequence-learning and retrieval network underlying spatial navigation.

Predictive Capability of the Model

The bifurcation curves shown in Figures 5 and 6 provide a concise and graphic description of the effect of manipulating the values of the connection strengths between the four cell populations in the model feedback circuit on its limit cycle behavior. If this model is an accurate, though coarse-grained, representation of the septal-hippocampal feedback circuit, then the bifurcation curves also provide a prediction of the effect on hippocampal theta of experimentally varying the connection strengths in the biological circuit, if physiologically possible.

Limitations of the Model

Our current model does not incorporate a number of important additional features of the anatomical feedback circuit. This is because we wished here to consider only a minimal computational model which was sufficient to demonstrate robust, theta-frequency oscillatory behavior, and yet simple enough to allow us to carry out a comprehensive bifurcation analysis of this behavior. In particular, we did not model the cholinergic neurons in the ms-dBB, which are also the target of the same hippocampal projections which terminate on the PV-containing inhibitory cells. These cholinergic neurons project to the pyramidal cells of the CA1 and CA3 regions of the hippocampus, where they have an excitatory effect on the latter cells, either directly or through a presynaptic termination on the inhibitory synapses on pyramidal cells formed by the feedback or feedforward interneurons in these regions (Freund and Gulyas, 1997; Levey et al., 1995). The cholinergic projection cells also strongly affect excitatory synaptic transmission, as well as inhibitory synaptic transmission, in CA1 and CA3 (Hasselmo et al., 1995), as also noted above. Within the medial septum, they are also reciprocally connected to the GABAergic septo-hippocampal projection cells.

Also, we did not model the PV-containing, hippocampal interneuron populations and the projections which the GABAergic ms-dBB neurons make on them. It is thought that these populations are involved in substantially distinct inhibitory circuits to those of the CB-containing nonpyramidal cells (Gulyas et al., 1991), and are probably significant in the maintenance of synchronous activity among hippocampal pyramidal and granule cells in the gamma frequency range (40–100 Hz) during each theta cycle (Chrobak and Buzsaki, 1998). The introduction of PV-containing cells in an extended model that we examined (unpublished) does not alter the fundamental theta frequency dynamic characteristics of the feedback circuit model as described here.

The circuit as proposed only considers the feedback interaction between ms-dBB and the CA1 region, whereas there are also strong GABAergic septal projections to CA3 interneurons (Freund and Antal, 1988), probably stronger than those to CA1 interneurons. We examined an extended model (unpublished) which includes these projections, in which we also modeled the CA3 pyramidal-cell population. In this model we postulated the target CA3 interneurons as feedback interneurons, and we showed that this has little effect on the dynamics of the feedback circuit as described in this paper. The effect is simply to drive the CA3 pyramidal cells in an oscillatory manner, which then makes the input P_{CA3} to the feedback circuit, as originally described, oscillatory. This simply reinforces the resulting stable limit cycle dynamic behavior, and the bifurcation diagrams are virtually unchanged.

A further enhancement to the circuit would be to include a direct projection back from the projection cell population in ms-dBB, to the hippocampo-septal projection cells in CA1, rather than just to the CA1 interneurons. This brings the circuit closer to that originally proposed by Toth et al. (1993), where this direct, monosynaptic feedback path was first identified. The effect of modifying the circuit in this way, for two different strengths of this connections, is shown in Figure 9a,b. These simulations show that, if the

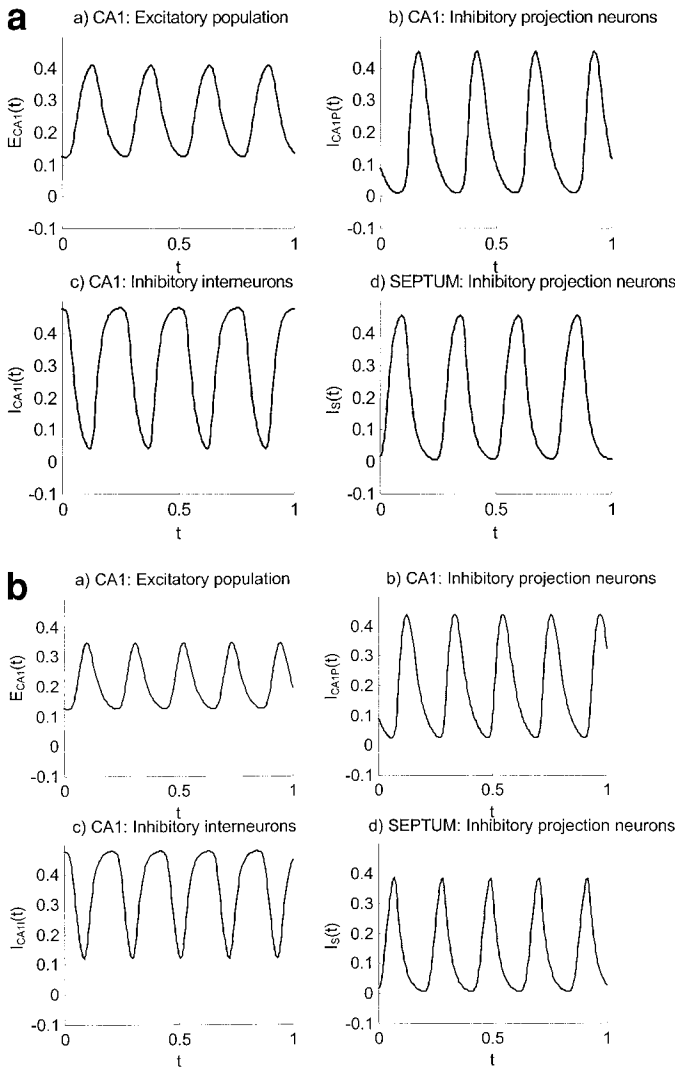


FIGURE 9. a: Effect on frequency of oscillation of the feedback circuit of including a direct feedback projection from the septo-hippocampal projection cells in ms-dBB to the hippocampo-septal projection cells in CA1, with a connection strength equal to 8, i.e., equal to that of the septal projection to the inhibitory interneuron population in CA1. Other parameter values are as in Table 1, with all time constants set at 30 ms. b: Effect on frequency of oscillation of the feedback circuit of including a direct feedback projection from the septo-hippocampal projection cells in ms-dBB to the hippocampo-septal projection cells in CA1, with a connection strength equal to 4, i.e., one half of that of the septal projection to the inhibitory interneuron population in CA1. Other parameter values are as in Table 1, with all time constants set at 30 ms.

connection strength is set equal to that of the septal projection to the CA1 interneuron population, the result is a reduction in the natural frequency of the circuit, from 6 Hz, as in Figure 2, to 4 Hz (Fig. 9a). If the connection strength is set to half that of the projection to the interneurons, the reduction in frequency of oscillation is to 5 Hz (Fig. 9b). Finally, further experiments show that increasing this connection strength from zero results in an almost linear falloff in oscillation frequency, up to a particular value of connection strength (for the set of parameter values in Table 1, this

value is around 10, i.e., about 25% greater than the strength of the septal projection to the interneurons). At this value the frequency falls off rapidly, from 3.5 Hz at a connection strength of 10, to zero (no oscillations) at a connection strength of 11.5 and greater. These results therefore appear to further enhance the validity of our claim that the feedback circuit plays a major role in the production of the GABA-mediated low-frequency rhythmic behavior of the septo-hippocampal system.

We also made a preliminary bifurcation analysis of this extended version of the circuit, and interestingly, the picture is more complicated. In addition to the supercritical Andronov-Hopf bifurcations, which alone exist in the original circuit, there are now subcritical Andronov-Hopf and other forms of bifurcation. From these initial studies, it appears that there is still a large region of the model parameter space in which there exists a stable limit cycle at theta frequency. However, further bifurcations exist, leading to other forms of oscillatory behaviors, and these are the subject of our ongoing investigations.

Finally, the effect of the serotonergic projections to both ms-dBB neurons and hippocampal neurons has been postulated as a mechanism for the disruption of theta, and hence should form part of a comprehensive computational model of the production and elimination of hippocampal theta activity. Work is currently in progress to expand our model in all the above respects, and also to study the circuits involved using more fine-grained neuron models.

Acknowledgments

R.B. was partly supported by the Russian Foundation of Basic Research (grant 99-04-49112). We acknowledge the anonymous reviewers of earlier versions of this paper for their very helpful and constructive comments and suggestions.

REFERENCES

Ali AB, Deuchars J, Pawelzik H, Thomson AM. 1998. CA1 pyramidal to basket and bistratified cell EPSPs: dual intracellular recordings in rat hippocampal slices. *J Physiol (Lond)* 507:201-217.
 Alonso A, Kohler C. 1982. Evidence for separate projections of hippocampal pyramidal and nonpyramidal neurons to different parts of the septum in rat brain. *Neurosci Lett* 31:209-214.
 Apartis E, PoindessousJazat FR, Lamour YA, Bassant MH. 1998. Loss of rhythmically bursting neurons in rat medial septum following selective lesion of septohippocampal cholinergic system. *J Neurophysiol* 79:1633-1642.
 Banks MI, Pearce RA. 2000. Kinetic differences between synaptic and extrasynaptic GABA_A receptors in CA1 pyramidal cells. *J Neurosci* 20:937-948.
 Banks MI, Tong-Bin L, Pearce RA. 1998. The synaptic basis of GABA_{A,slow}. *J Neurosci* 18:1305-1317.
 Bland BH, Oddie SD, Colom LV, Vertes RP. 1994. Extrinsic modulation of medial septal cell discharges by the ascending brainstem hippocampal synchronizing pathway. *Hippocampus* 4:649-660.
 Bland BH, Konopacki J, Kirk JJ, Oddie SD, Dickson CT. 1995. Discharge patterns of hippocampal theta-related cells in the caudal diencephalon of the urethane anaesthetized rat. *J Neurophysiol* 74:322-333.

- Bland BH, Trepel C, Oddie SD, Kirk IJ. 1996. Intraseptal microinfusion of muscimol: effects on hippocampal formation theta field activity and phasic theta-ON cell discharges. *Exp Neurol* 138:286–297.
- Bland BH, Oddie SD, Colom LV. 1999. Mechanisms of neural synchrony in the septohippocampal pathways underlying hippocampal theta generation. *J Neurosci* 19:3223–3237.
- Blasco-Ibanez JM, Freund TF. 1995. Synaptic input of horizontal interneurons in stratum oriens of the hippocampal CA1 subfield: structural basis of feed-back activation. *Eur J Neurosci* 7:2170–2180.
- Borhegyi Z, Magloczky Z, Acsady L, Freund TF. 1998. The supramammillary nucleus innervates cholinergic and GABAergic neurons in the medial septum-diagonal band of Broca complex. *Neuroscience* 82:1053–1068.
- Borisyuk RM, Kirillov AB. 1992. Bifurcation analysis of a neural network model. *Biol Cybern* 66:319–325.
- Borisyuk R, Denham M, Denham S, Hoppensteadt F. 1999. Computational models of predictive and memory-related functions of the hippocampus. *Rev Neurosci* 10:213–232.
- Brauer K, Seeger G, Hartig W, Rossner S, Poethke R, Kacza J, Schliebs R, Bruckner G, Bigl V. 1998. Electron microscopic evidence for a cholinergic innervation of GABAergic parvalbumin-immunoreactive neurons in the rat medial septum. *J Neurosci Res* 54:248–253.
- Brazhnik ES, Fox SE. 1997. Intracellular recordings from medial septal neurons during hippocampal theta rhythm. *Exp Brain Res* 114:442–453.
- Buhl EH, Halasy K, Somogyi P. 1994. Diverse sources of hippocampal unitary inhibitory postsynaptic potentials and the number of synaptic release sites. *Nature* 368:823–828.
- Buhl EH, Szilagy T, Halasy K, Somogyi P. 1996. Physiological properties of anatomically identified basket and bistratified cells in the CA1 area of the rat hippocampus in vitro. *Hippocampus* 6:294–305.
- Buzsaki G, Chrobak JJ. 1995. Temporal structure in spatially organized neuronal assemblies: a role for interneuronal networks. *Curr Opin Neurobiol* 5:504–510.
- Chrobak JJ, Buzsaki G. 1998. Operational dynamics in the hippocampal-entorhinal axis. *Neurosci Biobehav Rev* 22:303–310.
- Csicsvari J, Hirase H, Czurko A, Mamiya A, Buzsaki G. 1999. Oscillatory coupling of hippocampal pyramidal cells and interneurons in the behaving rat. *J Neurosci* 19:274–287.
- Denham MJ, McCabe SL. 1996. The biological basis for a neural model of learning and recall of goal directed sensory-motor behaviours. In: *Proceedings of the World Congress on Neural Networks (WCNN'96)*, San Diego. p 1283–1286.
- Denham MJ, McCabe SL. 1998. A model of predictive learning in the rat hippocampal principal cells during spatial activity. In: Simpson P, editor. *Proceedings of the IEEE International Joint Conference on Neural Networks (IJCNN'98)*. New York: Institute of Electrical and Electronic Engineering Press. p 1547–1552.
- Freund TF, Antal M. 1988. GABA-containing neurons in the septum control inhibitory interneurons in the hippocampus. *Nature* 336:170–173.
- Freund TF, Gulyas AI. 1997. Inhibitory control of GABAergic interneurons in the hippocampus. *Can J Physiol Pharmacol* 75:479–487.
- Gaykema RP, van der Kuil J, Hersh LB, Luiten PG. 1991. Patterns of direct projections from the hippocampus to the medial septum-diagonal band complex: anterograde tracing with *Phaseolus vulgaris* leucoagglutinin combined with immunohistochemistry of choline acetyltransferase. *Neuroscience* 43:349–360.
- Green JD, Arduini AA. 1954. Hippocampal electrical activity in arousal. *J Neurophysiol* 17:533–554.
- Gulyas AI, Freund TF. 1996. Pyramidal cell dendrites are the primary targets of calbindin D28k-immunoreactive interneurons in the hippocampus. *Hippocampus* 6:525–534.
- Gulyas AI, Gorcs TJ, Freund TF. 1990. Innervation of different peptide-containing neurons in the hippocampus by GABAergic septal afferents. *Neuroscience* 37:31–44.
- Gulyas AI, Toth K, Danos P, Freund TF. 1991. Subpopulations of GABAergic neurons containing parvalbumin, calbindin D28k, and cholecystokinin in the rat hippocampus. *J Comp Neurol* 312:371–378.
- Halasy K, Buhl EH, Lorinczi Z, Tamas G, Somogyi P. 1996. Synaptic target selectivity and input of GABAergic basket and bistratified interneurons in the CA1 area of the rat hippocampus. *Hippocampus* 6:306–329.
- Hasselmo ME, Schnell E. 1994. Laminar selectivity of the cholinergic suppression of synaptic transmission in rat hippocampal region CA1: computational modelling and brain slice physiology. *J Neurosci* 14:3898–3914.
- Hasselmo ME, Schnell E, Barkai E. 1995. Dynamics of learning and recall at excitatory recurrent synapses and cholinergic modulation in rat hippocampal region CA3. *J Neurosci* 15:5249–5262.
- Hasselmo ME, Wyble BP, Wallenstein GV. 1996. Encoding and retrieval of episodic memories: role of cholinergic and GABAergic modulation in the hippocampus. *Hippocampus* 6:693–708.
- Kawaguchi Y, Hama K. 1988. Physiological heterogeneity of nonpyramidal cells in rat hippocampal CA1 region. *Exp Brain Res* 72:494–502.
- Khibnik A, Kuznetsov Y, Levitin V, Nikolaev E. 1993. Continuation techniques and interactive software for bifurcation analysis of ODEs and iterated maps. *Physica D* 62:360–371.
- Kirk IJ. 1998. Frequency modulation of hippocampal theta by the supramammillary nucleus, and other hypothalamo-hippocampal interactions: mechanisms and functional implications. *Neurosci Biobehav Rev* 22:291–302.
- Kirk IJ, McNaughton N. 1993. Mapping the differential effects of procaine on frequency and amplitude of reticularly elicited hippocampal rhythmical slow activity. *Hippocampus* 3:517–525.
- Kirk IJ, Oddie SD, Konopacki J, Bland BH. 1996. Evidence for differential control of posterior hypothalamic, supramammillary, and medial mammillary theta-related cellular discharge by ascending and descending pathways. *J Neurosci* 16:5547–5554.
- Lee MG, Chrobak JJ, Sik A, Wilet RG, Buzsaki G. 1994. Hippocampal theta activity following selective lesion of the septal cholinergic system. *Neuroscience* 62:1033–1047.
- Leranth C, Frotscher M. 1989. Organization of the septal region in the rat brain: cholinergic—GABAergic interconnections and termination of hippocampo-septal fibers. *J Comp Neurol* 289:304–314.
- Leranth C, Deller T, Buzsaki G. 1992. Intraseptal connections redefined: lack of a lateral to medial septal path. *Brain Res* 583:1–11.
- Levey AI, Edmunds SM, Koliatsos V, Wiley RG, Heilman CJ. 1995. Expression of m1–m4 muscarinic acetylcholine receptor proteins in rat hippocampus and regulation by cholinergic innervation. *J Neurosci* 15:4077–4092.
- McLennan H, Miller JJ. 1974. The hippocampal control of neuronal discharges in the septum of the rat. *J Physiol [Lond]* 237:607–624.
- McLennan H, Miller JJ. 1976. Frequency-related inhibitory mechanisms controlling rhythmical activity in the septal area. *J Physiol [Lond]* 254:827–841.
- McNaughton N, Logan B, Panickar KS, Kirk IJ, Pan WX, Brown NT, Heenan A. 1995. Contribution of synapses in the medial supramammillary nucleus to the frequency of hippocampal theta rhythm in freely moving rats. *Hippocampus* 5:534–545.
- Miettinen R, Freund TF. 1992. Convergence and segregation of septal and median raphe inputs onto different subsets of hippocampal inhibitory interneurons. *Brain Res* 594:263–272.
- Petsche H, Gogolak G, Van Zwieten PA. 1965. Rhythmicity of septal cell discharges at various levels of reticular excitation. *Electroencephalogr Clin Neurophysiol* 19:25–33.
- Sik A, Penttonen M, Ylinen A, Buzsaki G. 1995. Hippocampal CA1 interneurons: an in vivo intracellular labeling study. *J Neurosci* 15:6651–6665.
- Stewart M, Fox SE. 1989a. Two populations of rhythmically bursting neurons in rat medial septum are revealed by atropine. *J Neurophysiol* 61:982–993.

- Stewart M, Fox SE. 1989b. Detection of an atropine-resistant component of the hippocampal theta rhythm in urethane-anaesthetized rats. *Brain Res* 500:55–60.
- Stumpf C. 1965. The fast component in the electrical activity of rabbit's hippocampus. *Electroencephalogr Clin Neurophysiol* 18:477–486.
- Sohal VS, Hasselmo ME. 1998a. Changes in GABA_B modulation during a theta cycle may be analogous to the fall of temperature during annealing. *Neural Comput* 10:869–882.
- Sohal VS, Hasselmo ME. 1998b. GABA(B) modulation improves sequence disambiguation in computational models of hippocampal region CA3. *Hippocampus* 8:171–193.
- Thinschmidt JS, Kinney GG, Kocsis B. 1995. The supramammillary nucleus: is it necessary for the mediation of hippocampal theta rhythm? *Neuroscience* 67:301–312.
- Thomson AM, West DC, Hahn J, Deuchars J. 1996. Single axon IPSPs elicited in pyramidal cells by three classes of interneurons in slices of rat neocortex. *J Physiol (Lond)* 496:81–102.
- Toth K, Freund TF. 1992. Calbindin D28k-containing nonpyramidal cells in the rat hippocampus: their immunoreactivity for GABA and projection to the medial septum. *Neuroscience* 49:793–805.
- Toth K, Borhegyi Z, Freund TF. 1993. Postsynaptic targets of GABAergic hippocampal neurons in the medial septum–diagonal band of Broca complex. *J Neurosci* 13:3712–3724.
- Toth K, Freund TF, Miles R. 1997. Disinhibition of rat hippocampal pyramidal cells by GABAergic afferents from the septum. *J Physiol (London)* 500:463–474.
- Tsodyks M, Skaggs W, Sejnowski T, McNaughton B. 1997. Paradoxical effects of external modulation of inhibitory interneurons. *J Neurosci* 17:4382–4388.
- Vertes RP, Kocsis B. 1997. Brainstem-diencephalo-septohippocampal systems controlling the theta rhythm of the hippocampus. *Neuroscience* 81:893–926.
- Vinogradova OS. 1995. Expression, control, and probable functional significance of the neuronal theta-rhythm. *Prog Neurobiol* 45:523–583.
- Walsh TJ, Stackman RW, Emerich DF, Taylor LA. 1993. Intraseptal injection of GABA and benzodiazepine receptor ligands alters high-affinity choline transport in the hippocampus. *Brain Res Bull* 31:267–271.
- Wilson HR, Cowan JD. 1972. Excitatory and inhibitory interactions in localized populations of model neurons. *Biophys J* 12:1–24
- Witter MP, Daelmans HEM, Jorritsma-Byham B, Staiger JF, Wouterlood FG. 1992. Restricted origin and distribution of projections from the lateral to the medial septal complex in rat and guinea pig. *Neurosci Lett* 148:164–168.

APPENDIX

Andronov-Hopf Bifurcation

In this Appendix we first give an intuitive explanation of the Andronov-Hopf bifurcation without mathematical details and formulas. Then we introduce a mathematical description of the Andronov-Hopf bifurcation. It is convenient to explain the main ideas for a general system of differential equations, and after that to relate these to the particular model Equations (1)–(4) which we consider in this paper.

Intuitive explanation

The mathematical model in Equations (1)–(4) describes the dynamics of the activity of four neural populations. This model is a deterministic system, which means that fixing the initial condi-

tions of the activities of each neural population at zero time completely defines all further dynamic behavior of this system. We can imagine the evolution of the activities of the system from zero time onwards as the movement of some “representing point” (current point) of the system in a four-dimensional (4-D) coordinate space relating to the four activity variables. This space is called as a “phase space.” The movement of the representing point is under the control of the dynamic system in Equations (1)–(4). This movement in time gives the trajectory in the phase space. Each trajectory is completely defined by the choice of the initial point (at zero time) in the phase space, and trajectories do not intersect each other. For example, Figure 4 shows a particular trajectory (closed curve) in 4-D phase space, projected into different 3-D subspaces.

There is a very important trajectory among all possible trajectories: it is the so-called equilibrium point (or fixed point, or steady state, or stationary point). The trajectory is an equilibrium point if the current position of the “representing point” at all times from zero onwards coincides with the initial position. This means that the “representing point” does not move in the phase space but stays at the initial position, and the activity of each neural population is stationary (constant in time).

The equilibrium point is stable if any trajectory starting from an initial point within a small neighborhood of the equilibrium point (i.e., close to this point) tends to the equilibrium point in time. In other words, any small perturbation of the system “representing point” from the stable equilibrium point decays to zero with time. The stable equilibrium point is often called an attractor, or sink, because it attracts all trajectories from within a small neighborhood around the equilibrium point. The equilibrium point is unstable if any small perturbation of the system from this point does not decay in time. An unstable equilibrium point is often called a repeller, or source.

We consider the model in Equations (1)–(4) under the condition that all parameters are fixed. Now let us suppose that we can vary one parameter (e.g., P_S) and keep all other parameters fixed (e.g., at the values in Table 1). Let us suggest that for $P_S = 25$, a stable equilibrium point exists in the phase space of the model in Equations (1)–(4). What happens to the stable equilibrium point if we vary the value of this parameter? If we change the parameter value by a small amount, then the coordinates of the equilibrium point will also change by a small amount, and it is likely that the stability of the point will be unchanged. Here we are interested in a qualitative behavior of trajectories of the model; the variation of the coordinates of the equilibrium point is not important. The qualitative picture only is important: all trajectories from a small neighborhood tend to the equilibrium point. Varying the parameter value, it is possible that qualitative picture is changed and that some (or all) trajectories do not tend to the equilibrium point. This means that the equilibrium point has lost its stability under the parameter variation. A critical parameter value when the equilibrium point loses its stability is called a bifurcation point. The bifurcation phenomenon corresponds to the qualitative rebuilding of trajectories pictured near the equilibrium point.

There are many different types of bifurcations. Here we consider the Andronov-Hopf bifurcation. The characteristic feature of the Andronov-Hopf bifurcation is that the equilibrium point loses its

stability and a new special trajectory appears. This special trajectory is a small closed curve (similar to a circle) and is called a limit cycle. If the initial value of the “representing point” is on the limit cycle, then for all times from zero onwards, the representing point moves along the curve, periodically returning to the initial point. Thus the activity of each population is periodically changing with time. These periodical changes are called oscillations. Thus, due to the Andronov-Hopf bifurcation, the equilibrium point loses its stability, and a small stable limit cycle appears nearby. The trajectories leave a small neighborhood of the unstable equilibrium point, and they tend to the stable limit cycle. This means that instead of stationary behavior, the model demonstrates oscillatory behavior. The equilibrium point is not an attractor anymore but a repeller, and the limit cycle is the only attractor. Sometimes the Andronov-Hopf bifurcation is called as the “limit cycle birth bifurcation.”

The amplitude of the oscillations which appear through the Andronov-Hopf bifurcation is small, but it increases when the parameter value deviates from the bifurcation point. The amplitude increases according to the “square root law” of the parameter deviation. For example, if the parameter deviation from the bifurcation point equals 0.01, then the value of amplitude is about 0.1. The period of oscillations depends on some features of the equilibrium point near the bifurcation, and it remains almost constant with the parameter deviation from the bifurcation point. Thus, the newborn oscillations have an amplitude which grows up promptly with the parameter deviation from the bifurcation point, and a period which is almost constant. The phenomenon of the Andronov-Hopf bifurcation is local, in the sense that all events are happening in a small neighborhood of the equilibrium point, and the description of the changes in amplitude and period of the oscillation is correct nearby the bifurcation point only (i.e., for small deviations of the parameter value from the bifurcation point). Further changes of the amplitude and period, when the parameter value is not very close to the bifurcation point, are under the control of another mechanism, different from the Andronov-Hopf bifurcation mechanism.

Now, let us suppose that all parameters of the model are fixed except two, say P_S and $w_{I_S \leftarrow I_{CA1}}$. On the plane of these two parameters there is a curve of Andronov-Hopf bifurcation points (Fig. 5a, top left). We can find this curve according to the following procedure. Suppose that the parameter P_S equals 25 and the value of the parameter $w_{I_S \leftarrow I_{CA1}}$ is varied in order to find the Andronov-Hopf bifurcation point. It means that on the plane $(P_S, w_{I_S \leftarrow I_{CA1}})$, we move the parameter $w_{I_S \leftarrow I_{CA1}}$ along the horizontal line $P_S = 25$, and on this line we can find the Andronov-Hopf bifurcation point $w_{I_S \leftarrow I_{CA1}} \approx 44$ (this point corresponds to the intersection of the horizontal line with the curve in Fig. 5a). The left part of this horizontal line corresponds to the values of $w_{I_S \leftarrow I_{CA1}}$ for which a stable equilibrium point exists, and the right part corresponds to the stable oscillatory regime. Repeating this procedure for other values of the parameter P_S (e.g., $P_S = 25.1, P_S = 25.2$, etc.), we can find other points on the bifurcation curve.

The bifurcation curve in Figure 5a is a boundary of the oscillatory region. Outside of this region, the equilibrium point is stable. Crossing the boundary at any point and in any direction, moving from outside the oscillatory region to inside, results in the An-

dronov-Hopf bifurcation: the equilibrium point loses stability and a stable limit cycle appears. If we choose any values of the parameters P_S and $w_{I_S \leftarrow I_{CA1}}$ inside of the oscillatory region (the values of other parameters are fixed according to the Table 1), then we will see oscillations because the equilibrium point is unstable and the only attractor is the stable limit cycle.

General theory

Let us propose that a model is described by a general system of n differential equations with n variables x_1, x_2, \dots, x_n and p parameters $(\alpha_1, \alpha_2, \dots, \alpha_p)$:

$$\begin{aligned} \frac{dx_1}{dt} &= f_1(x_1, x_2, \dots, x_n; \alpha_1, \alpha_2, \dots, \alpha_p), \\ \frac{dx_2}{dt} &= f_2(x_1, x_2, \dots, x_n; \alpha_1, \alpha_2, \dots, \alpha_p), \\ &\dots \\ \frac{dx_n}{dt} &= f_n(x_1, x_2, \dots, x_n; \alpha_1, \alpha_2, \dots, \alpha_p). \end{aligned} \tag{A1}$$

One can easily relate the general model (A1) with the particular model of the septal-hippocampal circuit in Equations (1)–(4). In this particular model we have four variables ($E_{CA1}, I_{CR1P}, I_{CA1F}, I_S$) corresponding to (x_1, x_2, x_3, x_4) , respectively; there are four differential equations and eleven parameters. Functions (f_1, f_2, f_3, f_4) relate to the right-hand side functions of the system in Equations (1)–(4) (normalized by the corresponding values of the time constant parameters τ).

It is convenient to use vector and matrix notations and re-write the system of differential Equations (A1) in a vector form

$$\frac{dx}{dt} = f(x; \alpha). \tag{A2}$$

Here $x = (x_1, x_2, \dots, x_n)$, $\alpha = (\alpha_1, \alpha_2, \dots, \alpha_p)$, and

$$\begin{aligned} f(x; \alpha) = & \\ & (f_1(x_1, x_2, \dots, x_n; \alpha_1, \alpha_2, \dots, \alpha_p), \\ & f_2(x_1, x_2, \dots, x_n; \alpha_1, \alpha_2, \dots, \alpha_p), \dots \\ & f_n(x_1, x_2, \dots, x_n; \alpha_1, \alpha_2, \dots, \alpha_p)). \end{aligned}$$

The vector x^0 is an equilibrium point (steady state, fixed point) for some parameter value α if x^0 is a solution of the following equation:

$$f(x^0; \alpha) = 0. \tag{A3}$$

Remark. The system (A3) could have more than one solution. This means that the model has several coexisting equilibrium points. Also, system (A3) could have no solutions at all, meaning that the model has no equilibrium points.

Let us consider some particular equilibrium point x^0 of the system (A2), which exists for parameter values $\alpha = \alpha^0$. This equilibrium point is stable (asymptotically stable) if any trajectory with an initial value within a small neighborhood of the equilibrium point tends to this equilibrium point in time.

There is a useful criterion to find whether the equilibrium point is stable or not. To use this criterion we need to find a matrix of partial derivatives of the right hand side of the system (A2) and calculate the values of these derivatives at the point $\alpha = \alpha^0, x = x^0$.

$$J = \begin{pmatrix} \frac{df_1}{dx_1} & \frac{df_1}{dx_2} & \dots & \frac{df_1}{dx_n} \\ \frac{df_2}{dx_1} & \frac{df_2}{dx_2} & \dots & \frac{df_2}{dx_n} \\ \dots & \dots & \dots & \dots \\ \frac{df_n}{dx_1} & \frac{df_n}{dx_2} & \dots & \frac{df_n}{dx_n} \end{pmatrix}$$

This matrix J is the linearization matrix of the system (A2), and the matrix $J^0 = J(x^0; \alpha^0)$ is the Jacobian matrix of the system (A2) at the equilibrium point $x = x^0$.

Criterion of stability by linear approximation. The equilibrium point $x = x^0$ is stable (in respect of a linear approximation of the system) if and only if all the eigenvalues of the Jacobian matrix J^0 are negative or, if they have complex values, if their real parts are negative. In other words, all eigenvalues $\lambda_1, \lambda_2, \dots, \lambda_n$ are in the left side of the complex plane (on the left of the imaginary axis): $\text{Re}(\lambda_m) < 0, m = 1, 2, \dots, n$.

If at least one eigenvalue has a real part outside of the left part of complex plane, i.e., is zero or positive, then the equilibrium point is unstable, i.e., there is a trajectory which does not tend to the equilibrium point with time.

Let us suppose that we keep all the parameters of system (A2) fixed except for one parameter, which we denote as β . A variation of this parameter results in a variation of the coordinates of the equilibrium point: $x^0 = x^0(\beta)$ (a small variation of the parameter value corresponds to a small variation of the coordinates). For any particular parameter value, we can find the stability of the equilibrium point $x^0 = x^0(\beta)$ by calculating the eigenvalues of the Jacobian matrix. Suppose that for $\beta = \beta^0$ the equilibrium point is stable, i.e., $\text{Re}(\lambda_m) < 0, m = 1, 2, \dots, n$, and under the parameter variation the equilibrium point loses its stability in such a way that a pair of complex-conjugate eigenvalues crosses the imaginary axis from the left to the right. The critical parameter value we denote by β^* and the Jacobian matrix of the equilibrium point $x^0 = x^0(\beta^*)$ has all its eigenvalues in the left side of complex plane, except for one pair which is exactly on the imaginary axis:

$$\lambda_{1,2} = 0 \pm i\omega, \quad \text{Re}(\lambda_m) < 0, m = 3, 4, \dots, n.$$

This means that the stability criterion has failed. This phenomenon, when we can see qualitative changes in dynamics (i.e., a stable equilibrium point becomes unstable), is called a bifurcation of the equilibrium point.

The critical parameter value $\beta = \beta^*$ and the corresponding coordinates of the equilibrium point $x^0(\beta^*)$ are called the bifurcation point. The particular bifurcation which we discuss here is called the Andronov-Hopf bifurcation. Let consider this bifurcation in more detail.

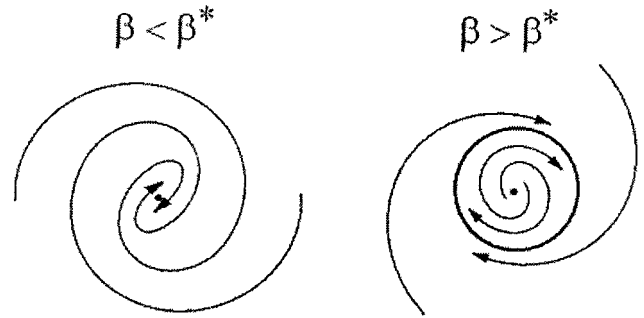


FIGURE A1. Trajectories of 2-D system in a small neighborhood of the equilibrium point for values of the parameter β less than or greater than its critical value β^* at the bifurcation point.

Remark. The Andronov-Hopf bifurcation phenomenon which we study here is local. It means that we consider parameter values and coordinates of the equilibrium point in a small neighborhood of the bifurcation point only.

Suppose that for the Andronov-Hopf bifurcation point $\beta = \beta^*, x^0(\beta^*)$, the equilibrium point is stable if $\beta < \beta^*$ and unstable if $\beta > \beta^*$. This means that for $\beta < \beta^*$, the trajectories of the system in a small neighborhood of equilibrium points look like spirals, with decaying amplitude of oscillations, and for $\beta > \beta^*$ the trajectories in a small neighborhood of equilibrium points look like spirals with increasing amplitude of oscillations (Fig. A1).

Where does the unstable spiral tend to with time? The Andronov-Hopf bifurcation is supercritical if for $\beta > \beta^*$ there is a special trajectory which looks like a small closed circle (this trajectory is called a limit cycle) and any trajectory from a small neighborhood of the equilibrium tends to the limit cycle. The limit cycle is stable if any trajectory from a small neighborhood of this limit cycle tends to the limit cycle with time. So, for the supercritical Andronov-Hopf bifurcation point $\beta = \beta^*, x^0(\beta^*)$ have:

1. For $\beta > \beta^*$ the equilibrium point $x^0(\beta)$ is stable and any trajectories in a small neighborhood of this equilibrium tend to the equilibrium as a spiral with decaying amplitude.
2. For $\beta > \beta^*$ the equilibrium point is unstable and in a small neighborhood there exists a stable limit cycle (with shape similar to a circle); and any trajectory tends to the limit cycle with time. The limit cycle has been born at $\beta = \beta^*$ and it exists for $\beta > \beta^*$.
3. The size of the limit cycle (amplitude of oscillations) increases continuously from zero, proportional to $\sqrt{\beta - \beta^*}$, for β close to β^* .
4. The frequency of the oscillations is given approximately by $\omega = \text{Im}(\lambda_{1,2})$ and the period is therefore $T = 2\pi/\omega$, evaluated at $\beta = \beta^*$. This formula is exact at the birth of the limit cycle.

Now we consider the case with two active parameters $\beta = (\beta_1, \beta_2)$ and all other parameters fixed. Assume that a supercritical Andronov-Hopf bifurcation exists for $\beta = \beta^*$. Then on the plane of two parameters (β_1, β_2) there exists an Andronov-Hopf bifurcation curve, and the point $\beta = \beta^*$ belongs to this curve. This curve on the plane of parameters is a boundary between two regions: the first region contains a stable equilibrium point, which

becomes unstable after crossing the bifurcation curve. The second region contains the stable limit cycle and unstable equilibrium.

Application to the septal-hippocampal model

We now illustrate the application of the general theory of Andronov-Hopf bifurcation for the septal-hippocampal model described by Equations (1)–(4). Assume, for example, that we fix all parameter values as in Table 1 except for two parameters: $(P_S, w_{IS \leftarrow I_{CAIP}})$. Figure 5a (top left) shows the Andronov-Hopf bifurcation curve on the plane of these two parameters. This means that at any point on this curve, the Jacobian matrix of the corresponding equilibrium point has a pair of eigenvalues with real part equal to zero. To find this curve, we used the software package LOCBIF (Khibnik et al., 1993). This software allows us to find different bifurcation points and curves for different types of bifurcations with one, two, or three active parameters.

The bifurcation curve in Figure 5a separates two regions: the region where the equilibrium point is stable, and the oscillatory

region where the equilibrium point is unstable but the stable limit cycle exists. The first region relates to the steady-state (baseline or background) behavior of neural activity, and the second region relates to the theta-rhythm oscillatory behavior. Crossing the bifurcation curve via any particular path from the first region to the oscillatory region will result in birth of a limit cycle, with its period of oscillation in the theta range. We found that along this bifurcation curve, the imaginary part ω of the eigenvalues of the Jacobian of the system varies in narrow bounds, i.e., in the range 40.1–42.5. This means that the frequency of oscillations nearby to the bifurcation curve is in the range 6.4–6.8 Hz. We checked by a very large number of simulations of the model that inside of the oscillatory region, the frequency of the limit cycle stays within a similar range. We obtained similar results for all other bifurcation curves in Figures 5 and 6: the imaginary part of the eigenvalues varies in a limited range along the bifurcation curve, and the frequency of oscillations is kept in the theta rhythm range of 6–7 Hz, both near the bifurcation curve and inside the oscillatory region.